Albert-Ludwigs-Universität Freiburg im Breisgau

Master Thesis

Tracking a Mobile Receiver using the Unscented Kalman Filter

Author:
Joan Bordoy Andreu
Universitat Politècnica
de Catalunya (UPC)

Supervisor:
Prof. Dr. Christian Schindelhauer

Technische Fakultät
Lehrstuhl für Rechnernetze und Telematik
Institut fur Informatik

October 2013

Declaration of Authorship

I, Joan Bordoy Andreu, declare that this thesis titled, "Tracking a Mobile Receiver using the Unscented Kalman Filter" and the work presented in it are my own. I confirm that:

- Where any part of this thesis has previously been submitted for a degree or any other qualification at this University or any other institution, this has been clearly stated.
- Where I have consulted the published work of others, this is always clearly attributed.
- Where I have quoted from the work of others, the source is always given. With the exception of such quotations, this thesis is entirely my own work.
- I have acknowledged all main sources of help.
- Where the thesis is based on work done by myself jointly with others, I have made clear exactly what was done by others and what I have contributed myself.

Signed: _____

Date: _____

UNI FREIBURG

Abstract

Technische Fakultät
Institut fur Informatik

Telecommunications Engineering

Tracking a Mobile Receiver using the Unscented Kalman Filter

by Joan Bordoy Andreu

Indoor localization based on Time Difference of Arrival (TDOA) and Frequency Difference of Arrival (FDOA) has been a promising subject of study the last years. In this thesis, a moving target is tracked by receiving discrete signals from stationary beacons. These beacons are assumed to be small and inexpensive and they require no further communication. Moreover, they emit short discrete signals at regular intervals and are assumed to be distinguished. The interval can be different for each sender and they do not need to start emitting at the same time instant, they can be unsynchronized. The algorithm used to solve this situation is the unscented Kalman filter. First, an approach using only the TDOA or FDOA measurements is presented. Second, it is extended to the combination of both measurements. Finally, the performance of these algorithms is evaluated with multiple experiments such as changing the dimension of the space to three dimensions or changing the number of senders.

Acknowledgements

First of all I would like to thank to Christian Schindelhauer for giving me the opportunity to do this thesis at his chair. It has been a fascinating and rewarding experience.

Thanks to the PhD candidate Johannes Wendeberg, this thesis would not have been possible without his support and guidance.

Last but not least thanks to my home university supervisor, Miguel Ángel Lagunas for his advice and support, especially before starting the thesis. Furthermore, his lessons in array processing helped me to discover the interesting area of the localization systems.

Contents

Declaration of Authorship i

Abstract ii

Acknowledgements iii

1 Introduction 1

2 Related Work 4
Decca Navigator System . . . 5
Loran Navigation System . . . 7
Global Positioning System . . . 9
Sender Localization . . . 10

3 Problem Formulation 11
TDOA . . . 11
FDOA . . . 13

4 Probabilistic State Estimation 16
Kalman Filter . . . 17
Motion Model . . . 20
Sensor Models . . . 21
Unscented Kalman Filter . . . 21
Unscented Kalman Filter using only TDOA or FDOA Measurements . . . 22
Unscented Kalman Filter using TDOA and FDOA Measurements . . . 25

5 Evaluation and Discussion 27
Simulation . . . 27
TDOA . . . 29
FDOA . . . 29
TDOA and FDOA . . . 30
3 Dimensions . . . 31
Senders in 3D and Receiver in 2D . . . 32
Influence of the Temperature in the Error . . . 32
Influence of the Interval Length and the Number of Senders in the Error . . . 36

6 Conclusions and Perspectives **39**

Bibliography **43**

Chapter 1

Introduction

Nowadays, the GPS (Global Positioning System) is part of our lives and almost every smartphone is provided of it. While this is an accurate solution for outdoor scenarios, it lacks connectivity in indoor locations. A promising research topic is to find a reliable approach for this scenario, as many applications could benefit from it.

This master thesis took place in the context of the *eCULTS* project, which is a collaboration between academic and industrial partners to create a location system for indoor logistics. The goal is to create a system which minimises the cost and has a high availability at the same time. Furthermore, it is required to have an easy installation and to need low effort to be maintained by the customer. Precisely *eCULTS* is the acronym for **e**nergy-autarkic **C**alibration-free **UL**trasound **T**racking **S**ystem. The system is based on ultrasounds, as the beacons are cheap and their performance is usually better than the electromagnetism approaches, specially in adverse scenarios, where materials like silicone grease can deteriorate the transmission of electronic signals, as they are electrical isolators. On the contrary, these materials help to propagate the vibrations of the ultrasound. In fact, materials like motor oil and grease can be used as ultrasonic couplants [1].

In the traditional logistics of a commerce enterprise forklifts and manually operated cranes are used to transport and store goods. Another material handling equipment used are the conveyor belts. While they do not need an operator, they have a fixed trajectory. The aim of the *eCULTS* project, which started in October 2012, is that autonomous agents are able to transport goods based on dynamic assignments. The academic partners of the project are the Department of Computer Science (IFF) and the Department of Microsystems Engineering (IMTEK) of the university of Freiburg and it is funded by the German Federal Ministry of Education and Research (BMBF).

The localization techniques used are the TDOA (Time Difference of Arrival) and the FDOA (Frequency Difference of Arrival). This thesis presents an approach where the position of a moving receiver is tracked (see Fig. 1.1), in contrast to many TDOA algorithms which track the position of a moving sender. The target receives short signal bursts from a set of inexpensive ultrasound beacons, whose locations are assumed to be estimated beforehand with one of the algorithms cited in the related work. The signals are assumed to be identified and distinguished using a multiplex technique such as FDMA or CDMA and their intervals are assumed to be unknown in advance and can be different for every sender. Furthermore, the senders are assumed to be unsynchronized.

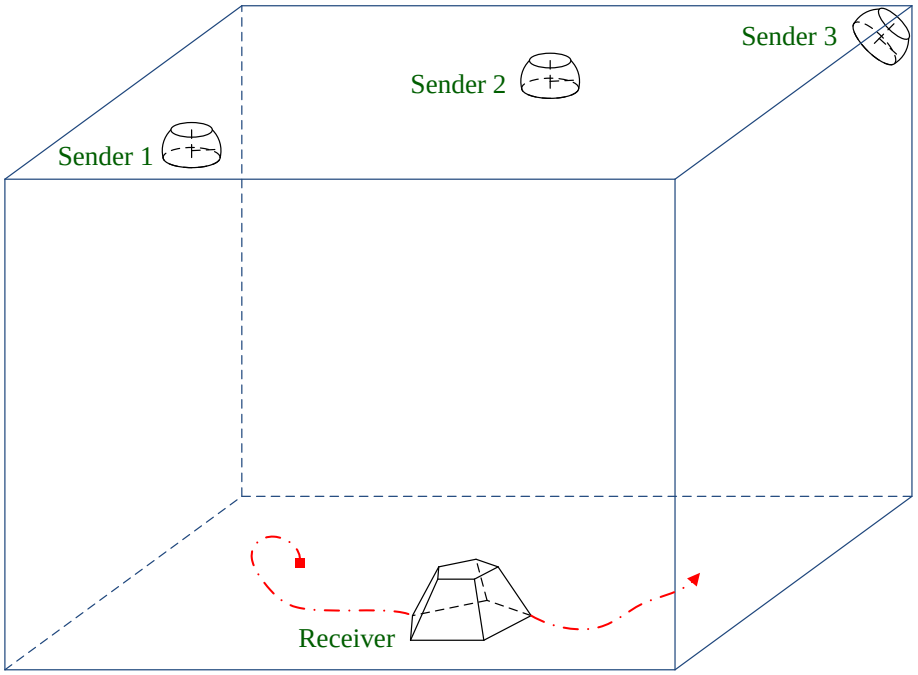

FIGURE 1.1: Schematic representation of the scenario when a receiver is moving in two dimensions and the receivers are located in a three-dimensional space.

This means the time differences of the first signal of the beacons are not determined, therefore, once the sender positions and the intervals are known there still remains an unknown offset. Besides, in practical applications appears the problem of the oscillator drift of the sender clocks which changes the offset of the senders.

As the receiver moves continuously between two measurements the number of unknown variables increases faster than the number of constrains causing a mathematical problem that can not be solved in a closed form. Due to this fact, we propose an approach based on probabilistic state estimation which recursively estimates the receiver position and

the sender offsets only by the reception times of the signals from the sender beacons. In particular, the unscented Kalman filter (UKF) is used, which is a computationally efficient recursive algorithm. Its performance is tested in Chapter 5 with multiple simulations in different scenarios. The Chapter 2 focuses on the related work and algorithms implemented by other authors to estimate the position of the senders. The Chapter 3 introduces the problem and explains the TDOA and FDOA techniques. Finally, the Chapter 4 details the implementation of the UKF algorithm.

Chapter 2

Related Work

The TDOA localization problem has been solved in many approaches with stationary receivers and a moving sender. The algorithms used are squared or maximum likelihood estimators [2], particle filters [3, 4] or Kalman filters [5, 6]

In some approaches the receivers are also moving with a known velocity. This knowledge is used to calculate the FDOA measurements, which are fused with the TDOA measurements. The sender to track can be either in motion [7–9] or fixed [10]. An approach in the presence of receiver location errors in which the sender is not fixed was presented in [11].

In mobile robotics some approaches use multiple sensors to detect and measure the landmarks of an environment. These measurements are combined and used to estimate the pose of the robot. In [12] this is solved with the unscented Kalman filter and the extended Kalman filter showing that the UKF has a slightly better performance. An approach where an iterative UKF is used to reduce the non linearities is presented in [13]. In [14] a combination of the UKF and the particle filter is presented.

The situation of locating a moving receiver has been solved with Time of Arrival(TOA) and Angle of Arrival (AOA) methods in [15]. They use a particle filter to estimate the position and adaptive fuzzy control to minimize the error. In [16] TDOA measurements are used to estimate the position of a target and the senders with the aid of the odometry measurements. The receiver is assumed to have a simple trajectory and is tracked with a weighted least squares procedure.

This master thesis is a continuation of the work done in [17], where the same situation presented here was solved by the particle filter with TDOA. The particle filter, also known as Monte Carlo localization, is a recursive algorithm which uses “particles” to

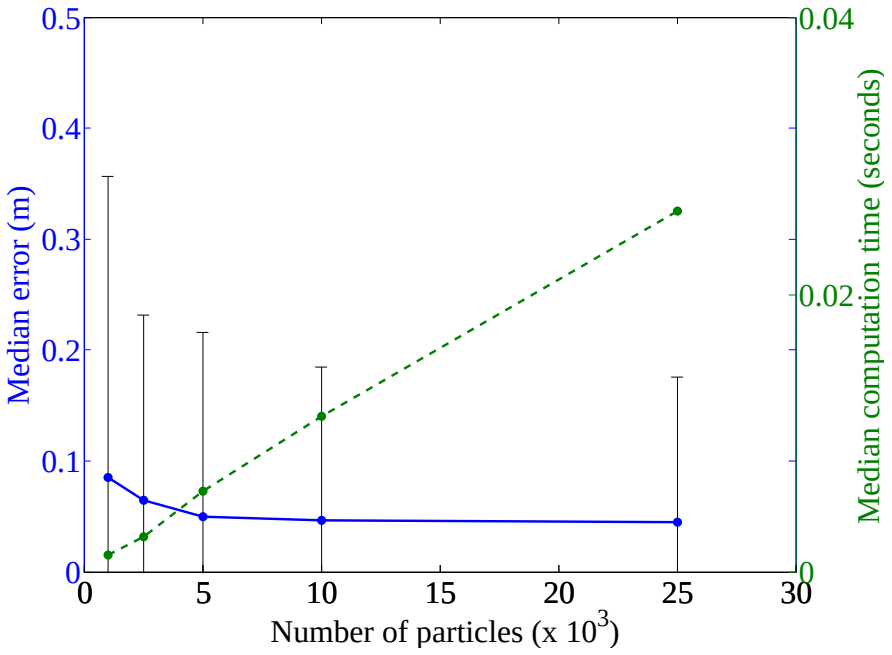

FIGURE 2.1: Effect of increasing the number of particles on the median error (solid line) and on the computation time (dotted line) of one cycle of the particle filter when a moving receiver is tracked by unsynchronized senders [19].

represent the hypothesis. Each particle is weighted depending on the probability distributions. Subsequently, in the resampling step, the particles with lower weights are replaced for new ones located near the particles with higher weights. The performance of this algorithm depends on the number of particles used and therefore the computational cost, as is shown in Fig. 2.1, where a moving sender was tracked with different numbers of particles measuring the median computation time of one cycle for each case. To achieve a reasonable error high number of particles are needed and therefore a high computation time [18]. In this thesis the UKF is used, which is more efficient computationally, taking advantage also of the FDOA measurements. Furthermore, it is extended to three dimensions.

Part of this thesis has been already published as an article in [19], where a moving receiver was tracked in two dimensions with the aid of the TDOA measurements using both the UKF and the particle filter and comparing them. It was shown that the particle filter has a slightly better performance with a higher computational cost.

Decca Navigator System

The Decca Navigator System comes from the low frequency phase comparison hyperbolic position-fixing technique invented in 1937 in the USA by Willem Joseph O'Brien to measure the ground speed of an aircraft [20]. Afterwards, it was used in the World

TABLE 2.1: Typical radiated and comparison frequencies in the Decca navigation system with f_R=14.16 kHz

	Harmonic	Frequency (kHz)	Wavelength (m)
Master	$6f_R$	85	3521
Red slave	$8f_R$	113.33	2640
Green slave	$9f_R$	127.500	2347
Purple slave	$5f_R$	70.833	4225
Red comparison	$24f_R$	340	880
Green comparison	$18f_R$	255	1174
Purple comparison	$30f_R$	425	704

War II under the codename QM for ship navigation in coastal waters and played an important role in the decisive allied victory of the Overlord operation. In 1945 it was released for commercial use under the name of Decca Navigator.

The basic system for marine applications [21] used pairs of master and slave stations. Having a master transmitting station A and a slave transmitting station B separated a distance S sending electromagnetic waves with the same frequency and locked in phase, the measured phase in a point at a distance r_A from the master and at a distance r_B from the slave is:

$$\Theta = \frac{2\pi}{\lambda}(S + r_A - r_B) \tag{2.1}$$

where λ is the wavelength of the signals. For a fixed measurement the position of the receiver is a hyperbola focused on the two transmitting stations. In practice, the signals of the master and the slave stations were sent with different frequencies so they could be distinguished by the receiver. Concretely, they were sent with harmonically-related frequencies. In the "red" pattern, given a reference frequency f, the master could use a frequency of $6f$ and the slave a frequency of $8f$. Afterwards the receiver multiplied the frequency of the slave by 4 and the frequency of the master by 3 resulting in a common frequency of $24f$. The usual frequencies used are shown in Table 2.1.

The values of the phase Θ for different pairs of slave and master were used to estimate the position of the ship in a map, which had the result of the hyperbolic equations for each possible measurement. The intersection of the lines of different pairs of stations resulted in the estimated position of the vessel, as it is shown in Fig. 2.2.

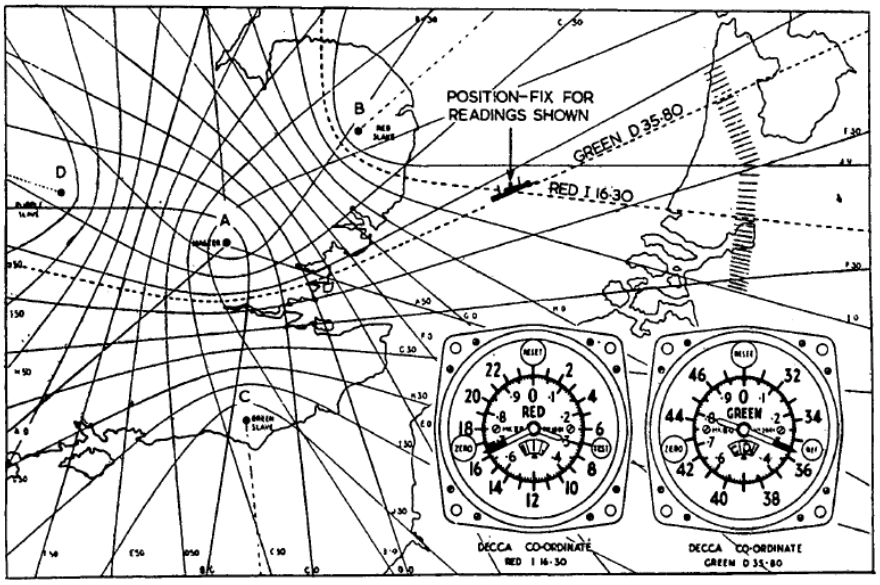

FIGURE 2.2: Representation of a Decca map [21]. The hyperbolas are drawn for different possible values of Θ and afterwards chosen depending on the measurements.

The phase angle of a cosine wave with respect to another is related with the time delay Δt as follows:

$$cos(2\pi ft + \Theta) = cos(2\pi f(t + \Delta t)) \tag{2.2}$$

$$2\pi ft + \Theta = 2\pi f(t + \Delta t) \tag{2.3}$$

$$\Theta = 2\pi f \Delta t \tag{2.4}$$

A cosine has all the energy in one single frequency in the frequency domain. Approximating the signals with low bandwidth as cosines one can say that, for narrow-band transmitters, the phase difference can be considered the same as the time difference (TDOA). Nevertheless, in this system the position has to be estimated manually depending on various measurements, while our approach uses the UKF to estimate one position for every received measurement. Another disadvantage is that the slave stations need to be phase-locked with the master station. This makes necessary a reference system which transmits the reference frequency f_R, as the phase can be shifted by the temperature or the analogue amplifiers.

Loran Navigation System

Loran, which is the acronym of **Lo**ng **Ra**nge **N**avigation, started to be implemented by the US Coast Guard in the World War II. After the war there were over 70 transmitters providing coverage over approximately 30% of the earth's surface [22]. Nowadays it is

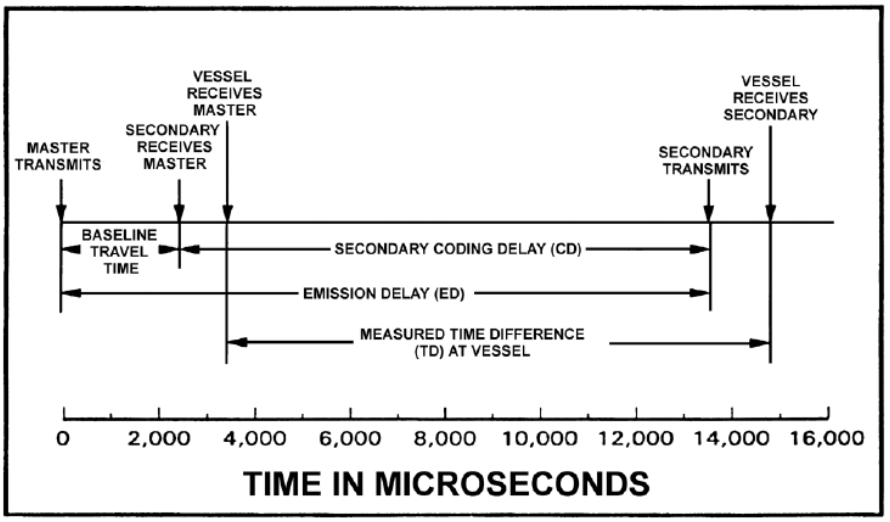

FIGURE 2.3: Time axis of a Loran transmission[22].

being replaced by the GPS, as evidenced by the fact that the USA and Canada terminated the transmission of all the Loran signals the 8 February 2010 [23]. Nevertheless there still remain some active stations in other countries like Norway, France, Saudi Arabia or India.

The Loran C, which is the most implemented version, uses transmitting stations organized into chains, where one of the stations is the master station and the others are secondary stations. The master station sends series of 100 kHz pulses, which are received by the vessel and by the secondary stations. Once the secondary stations receive the signal, they send it again after a certain coding delay t_{CD}, as it is shown in Fig. 2.3. The time difference between the received signals by the vessel is computed. Given a master station in $\mathbf{S}_M$ and a secondary station in $\mathbf{S}_s$ the time difference Δt can be written as follows:

$$\Delta t = \frac{1}{c}\|\mathbf{M} - \mathbf{S}_s\| + t_{CD} + \frac{1}{c}\|\mathbf{S}_s - \mathbf{S}_M\| - \frac{1}{c}\|\mathbf{M} - \mathbf{S}_M\| \tag{2.5}$$

where c is the speed of light, $\mathbf{M}$ is the position of the vessel and $\|\cdot\|$ denotes the Euclidean norm. As the position of the stations and the coding delay are assumed to be known, the locus of points where Δt is held constant is a hyperbolic position line, which crossed to other lines gives the position of the receiver. It can be either estimated by a computer algorithm or with a chart like the one used in Decca. While this approach does not need synchronized senders, the secondary stations need to receive and process signals, which has a higher economic cost than having stations which only send signals.

Global Positioning System

The Global Positioning System (GPS) is a radio positioning system developed by the U.S. Department of Defence which uses a constellation of 21 satellites to track the position of a receiver so as anywhere on the Earth there are at least four satellites in view at any time [23].

The components of this system are divided into three categories:

- Space segment: Consists of 21 operational satellites orbiting at an altitude of 20200 Km. Each satellite transmits signals with a frequency of 1575 MHz and 1227.6 MHz using a code division multiple access (CDMA) technique to identify itself. The signals contain information about predicted satellite ephemeris, atmospheric propagation correction data, satellite clock error information and satellite health data.
- Control segment: This segment consists of a master control station located in Colorado, U.S. and a set of monitor stations and ground antennas located throughout the world. The monitor stations track the performance of the satellites and relay the information to the master control station, which uses it to update the navigation messages of the satellites. These new messages are sent to the satellites with the aid of the ground antennas.
- User segment: This is the user equipment. It generates a timing signal at the same time as the satellite. Afterwards, the phase difference between these two signals and the information of the received navigation messages are used to estimate the distance to the satellite. The device can differ depending on the application but the most common algorithm used in the handheld GPS is the Kalman filter [24].

The Global Positioning System achieves an error of 1-5 meters in outdoor scenarios [25]. Having senders located in a room reduces this error, as the signals are less affected by the atmospheric effects and they are not affected by the ephemeris error of the satellite. Furthermore, to reach an indoor location the signals loose from 10 to 30 dB due to the attenuation of the microwaves caused by the walls. This requires the presence of indoor repeaters, as when the signals reach the earth surface they have a low power level (approximately 130 dBm).

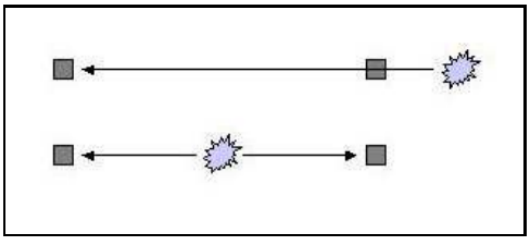

FIGURE 2.4: The maximum TDOA scenario and the minimum TDOA scenario are represented for two sensors receiving a signal [27]. The acoustic event is represented by a star and the sensors are represented by squares.

Sender Localization

As explained in the previous chapter, in this thesis the location of the senders is assumed to be known beforehand. Their position can be estimated with the Ellipsoid TDOA method, which uses the TDOA measurements to formulate an ellipsoid equation. In [26] a linear regression algorithm is used to estimate the position of a set of receivers with the aid of ambient signals. The precision of this method depends on the far field assumption, i.e., the receivers are assumed to be very far from the senders therefore having them too close can led to huge errors.

Some approaches [17, 27, 28] use the statistical distribution and the maximum and minimum of the timestamps received by the sensors to locate the pose of a set of receivers or senders. They take profit of the fact that when two sensors are aligned in the direction of propagation of one signal, the difference of the reception time between them is the maximum. This maximum multiplied by the ultrasound propagation velocity is their distance. The figure 2.4 shows the maximum TDOA scenario in the top view and a case where the TDOA is zero in the bottom view. The precision of these approaches depends on the availability of signals aligned with the receivers.

Chapter 3

Problem Formulation

The problem considered in this thesis is tracking a moving receiver on an unknown trajectory with the unscented Kalman filter. Is considered both the case when the receiver is moving in a two-dimensional space and the case when is moving in a three-dimensional space.

The scenario consists of m stationary senders placed in random positions $\mathbf{S}_i$ $(1 \leq i \leq m)$. The position of the receiver at time t is represented by the variable $\mathbf{M}_t$. Three cases are considered here: Two cases where the senders and the receiver vector have the same dimension (2D and 3D) and a case where the receiver is moving in a two-dimensional space and the senders are located in a three-dimensional space. Every sender emits discrete signals at regular points in time at a fixed interval I_i. The interval may differ from sender to sender.

The sending time of the k_i-th signal at sender position $\mathbf{S}_i$ is then described by

$$t_{k_i i} = t_{0i} + k_i I_i \ , \qquad (k_i > 0). \tag{3.1}$$

TDOA

This section is based on the work done in [17].

To estimate the position of the receiver the assumption made is that a k_i-th signal of sender $\mathbf{S}_i$ propagates in a straight line from the sender to the receiver and is received at time point

$$T_{k_i i} = \frac{1}{c}\|\mathbf{M} - \mathbf{S}_i\| + t_{k_i i}, \tag{3.2}$$

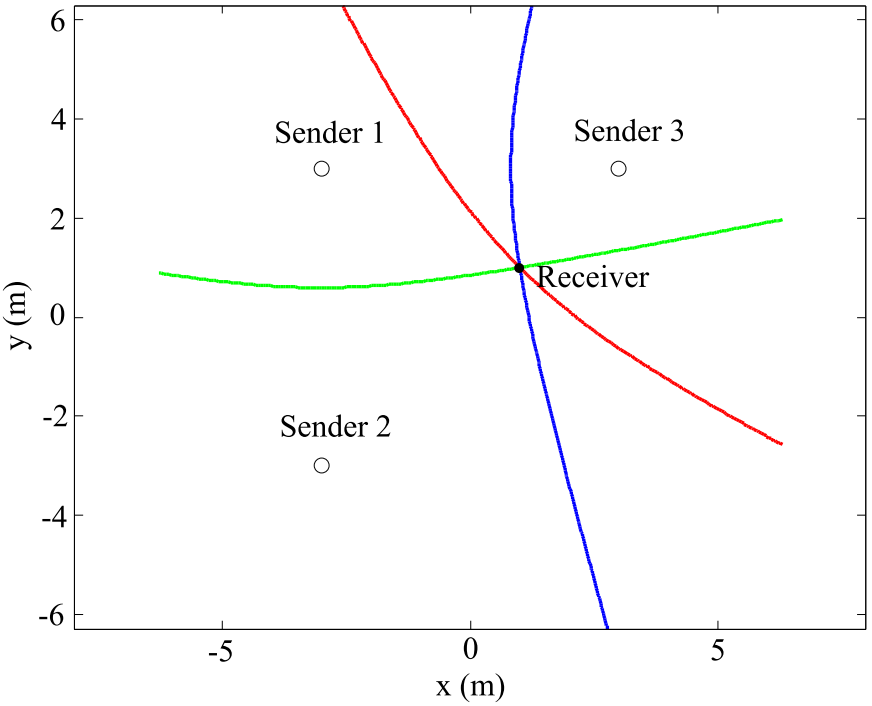

FIGURE 3.1: TDOA hyperbolic curves when the receiver is not moving between two measurements.

where c is the signal velocity and $\|\cdot\|$ denotes the Euclidean norm. Furthermore, we assume that the signals can be distinguished, as explained before.

First, let's consider that the target is not moving between two received signals. Comparing the timestamps from two senders we get an hyperbolic curve:

$$TDOA_{ij} = \frac{1}{c}\|\mathbf{M} - \mathbf{S}_i\| + t_{k_i i} - \frac{1}{c}\|\mathbf{M} - \mathbf{S}_j\| - t_{k_j j}, \tag{3.3}$$

With three senders three curves are obtained, whose intersection results in the position of the receiver, as is shown in Fig. 3.1. Note that in three dimensions one sender more is needed to estimate the altitude.

As in this thesis the receiver is assumed to be moving between two received signals, the TDOA can not be calculated just comparing the timestamps. Due to this assumption, to successfully compute the position of the receiver more effort is needed. Up to now only the signal speed c, the time when a signal has been received, T, and the position of the senders $\mathbf{S}_i$ are known.

The computation of the length of the intervals of the different senders by the receiver is straightforward by receiving two or more successive signals $k_1, k_2, k_1 \neq k_2$, emitted by

the same sender $\mathbf{S}_i$ while it is temporarily stationary. Then the interval for sender $\mathbf{S}_i$ is

$$I_i = \frac{1}{k_1 - k_2}(T_{k_1 i} - T_{k_2 i}) \, . \tag{3.4}$$

The senders are assumed to be unsynchronized, i.e. they send the signals after different intervals and have a different initial send time t_{0i}. Consequently, there is an unknown time offset δ_{ij} between the senders, which describes the send time difference between senders $\mathbf{S}_i$ and $\mathbf{S}_j$. It is calculated by

$$\delta_{ij} = t_{0i} - t_{0j} = (t_{k_i i} - k_i I_i) - (t_{k_j j} - k_j I_j) \, . \tag{3.5}$$

If all $\binom{m}{2}$ offsets are known or equal to zero, the senders are considered synchronized. Since the offsets are transitive, only $m - 1$ offsets must be computed, relative to one sender.

These assumptions result in the following hyperbolic equation in which two signals, originating from two different senders $\mathbf{S}_i$ and $\mathbf{S}_j$, are received at the positions $\mathbf{M}_{k_i i}$ and $\mathbf{M}_{k_j j}$:

$$\frac{1}{c}(\|\mathbf{M}_{k_i i} - \mathbf{S}_i\| - \|\mathbf{M}_{k_j j} - \mathbf{S}_j\|) = \Delta t_{ij} + \delta_{ij} \, , \tag{3.6}$$

where Δt_{ij} represents the unsynchronized time difference of arrival of the two signals originated by $\mathbf{S}_i$ and $\mathbf{S}_j$, which may be calculated based on the reception times and the intervals as

$$\Delta t_{ij} = (T_{k_i i} - T_{k_j j}) - (k_i I_i - k_j I_j) \, . \tag{3.7}$$

In this equation m is the number of senders, so $m - 1$ offsets are required. Assuming the intervals I_i and I_j and the positions of the receivers $\mathbf{S}_i$ $\mathbf{S}_j$ are known, there exist $2n + (m - 1)$ unknown variables after $2n$ received signals and therefore unknown receiver positions, see Fig. 3.2. One can see that this equation cannot be solved in closed form and without further knowledge and assumptions on the scenario.

FDOA

The Doppler effect, proposed by Christian Doppler [29], is the shift of the frequency for an observer moving relative to a source and provides useful information about their

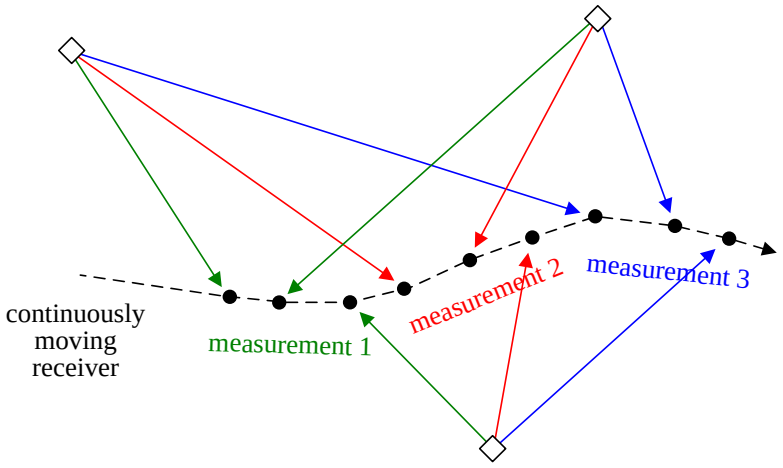

FIGURE 3.2: It is a schematic of the under-determined equation system [19]: Three senders (white diamonds) send three signals. The receiver moves continuously receiving the signals from each sender at nine unknown positions (black dots). This results in 18 unknown variables in 2D and 27 in 3D only for the receiver.

position. The equation is usually written as follows:

$$f = \left(\frac{c + v_r}{c + v_s}\right) f_0 \tag{3.8}$$

where f is the observed frequency by the receiver and v_r its velocity. The emitted frequency is noted as f_0 and the velocity of the source as v_s. The velocities are relative to the medium and their sign depends on whether they are moving towards or away from each other. The velocity of the receiver is positive if it is moving towards the sender and negative if it is moving away, contrary to the velocity of the sender, which is positive if it is moving away from the receiver and negative if it is moving towards.

In our case, the senders are stationary therefore their velocity is zero:

$$f = \left(\frac{c + v_r}{c}\right) f_0 \tag{3.9}$$

The frequency is the inverse of the period. In this case, the observed period is the difference of time between two consecutive timestamps of the same sender $(T_{k_i i} - T_{k-1_i i})$ and the emitted period is its interval I_i:

$$I_i = \left(\frac{c + v_r}{c}\right)(T_{k_i i} - T_{k-1_i i}) \longrightarrow I_i = T_{k_i i} - T_{k-1_i i} + \frac{(T_{k_i i} - T_{k-1_i i})v_r}{c} \tag{3.10}$$

The product of $T_{k_i i} - T_{k-1_i i}$ and v_r is the movement of the receiver during two timestamps. This can be also obtained from:

$$(T_{k_i i} - T_{k-1_i i})v_r = -(\|\mathbf{M}_{k_i i} - \mathbf{S}_i\| - \|\mathbf{M}_{k-1_i i} - \mathbf{S}_i\|) \tag{3.11}$$

which is a more robust equation, as it is adding the knowledge of the position of the sender to the equation. The negative sign has to be placed in the equation as the velocity of the receiver is defined positive if it is moving towards the source and negative if it is moving away from it.

Using the Eq. 3.11 in the Eq. 3.10:

$$T_{k_i i} - T_{k-1_i i} = \frac{1}{c}(\|\mathbf{M}_{k_i i} - \mathbf{S}_i\| - \|\mathbf{M}_{k-1_i i} - \mathbf{S}_i\|) + I_i \tag{3.12}$$

which is the equation used to measure the FDOA.

Chapter 4

Probabilistic State Estimation

As discussed in the chapter "Problem Formulation", the equation system in Eq. 3.6 is under-determined and cannot be calculated in a closed form. To solve this, the unscented Kalman filter is used. This filter is an implementation of the Bayesian filtering model, which is a probabilistic approach to recursive state estimation. This model is based on the assumptions that are detailed below.

The filter fulfils the Markov assumption, that is the current state only depends on the previous state:

$$p(\mathbf{x}_t|\mathbf{x}_{0:t-1}) = p(\mathbf{x}_t|\mathbf{x}_{t-1}) \tag{4.1}$$

To estimate the current state, a measurement $\mathbf{z}$ and a control variable u are used. The control variable is the only variable that relates the current state and the previous state:

$$p(\mathbf{x}_t|\mathbf{x}_{0:t-1}, \mathbf{z}_{1:t-1}, \mathbf{u}_{1:t}) = p(\mathbf{x}_t|\mathbf{x}_{t-1}, \mathbf{u}_t) \tag{4.2}$$

The measurement does not depend on the previous states, measurements or control variables, it can be predicted only with the current state:

$$p(\mathbf{z}_t|\mathbf{x}_{0:t}, \mathbf{z}_{1:t-1}, \mathbf{u}_{1:t}) = p(\mathbf{z}_t|\mathbf{x}_t) \tag{4.3}$$

Using all of these assumptions, the probability distribution of the current state depending on the measurements and controls can be written as follows:

$$p(\mathbf{x}_t \mid \mathbf{z}_{1:t}, \mathbf{u}_{1:t}) \;=\; \eta_t \, p(\mathbf{z}_t \mid \mathbf{x}_t) \int p(\mathbf{x}_t \mid \mathbf{u}_t, \mathbf{x}_{t-1}) p(\mathbf{x}_{t-1} \mid \mathbf{u}_{1:t-1}, \mathbf{z}_{1:t-1}) \, d\mathbf{x}_{t-1} \tag{4.4}$$

where the parameter η_t is a normalizing constant ensuring that $\int p(\mathbf{x}_t \mid \mathbf{u}_{1:t}, \mathbf{x}_{1:t}) \, d\mathbf{x}_t \;=\; 1$. The state transition probability $p(\mathbf{x}_t \mid \mathbf{u}_t, \mathbf{x}_{t-1})$ and the measurement probability $p(\mathbf{z}_t \;\mid\; \mathbf{x}_t)$

are specified by the motion model and sensor model respectively or by the A_t, B_t and C_t matrices depending on the type of Kalman filter used, as it is explained in the next sections.

In our case, the state consists of the position vector $\mathbf{M}_t$ of the receiver at time t, as well as the movement velocity of the receiver $\mathbf{V}_t$. Since the senders are unsynchronized, the time offsets δ_{ij} need to be estimated as well. Altogether, the state vector is

$$\mathbf{x}_t = \left(\mathbf{M}_t^T, \mathbf{V}_t^T, t_{k1}, \delta_1, ..., \delta_m\right)^T . \tag{4.5}$$

Kalman Filter

For better understanding, in this section the basic Kalman filter is explained, as the unscented Kalman filter is a modification of it.

The Kalman filter requires that the state transition probability $p(\mathbf{x}_t \mid \mathbf{u}_t, \mathbf{x}_{t-1})$ is a linear function in its arguments with added Gaussian noise:

$$\mathbf{x}_t = A_t\mathbf{x}_{t-1} + B_t\mathbf{u}_t + \varepsilon_t \tag{4.6}$$

where ε_t is the process noise. The matrix A_t has a dimension of $n \times n$, with n being the size of the state vector $\mathbf{x}_t$. The size of the matrix B_t is $n \times m$, where m is the size of the control vector $\mathbf{u}_t$.

The measurement probability $p(\mathbf{z}_t \mid \mathbf{x}_t)$ must be linear also in its arguments with added Gaussian noise. The measurement is predicted with the state as follows:

$$\mathbf{z}_t = C_t\mathbf{x}_t + \varphi_t \tag{4.7}$$

where φ is the measurement noise and C_t is a $k \times n$ matrix, being k the dimension of the measurement vector $\mathbf{z}_t$.

The first step of the algorithm is to predict the mean and the variance of the state, based on the previous belief, to propagate the state hypothesis in the current time step. This is done with the previous mean μ_{t-1} and covariance Σ_{t-1}, the control variable $\mathbf{u}_t$ and the covariance of the process noise R_t:

$$\begin{aligned} \overline{\mu_t} &= A_t\mu_{t-1} + B_t\mathbf{u}_t \\ \overline{\Sigma_t} &= A_t\Sigma_{t-1}A_t^T + R_t \end{aligned} \tag{4.8}$$

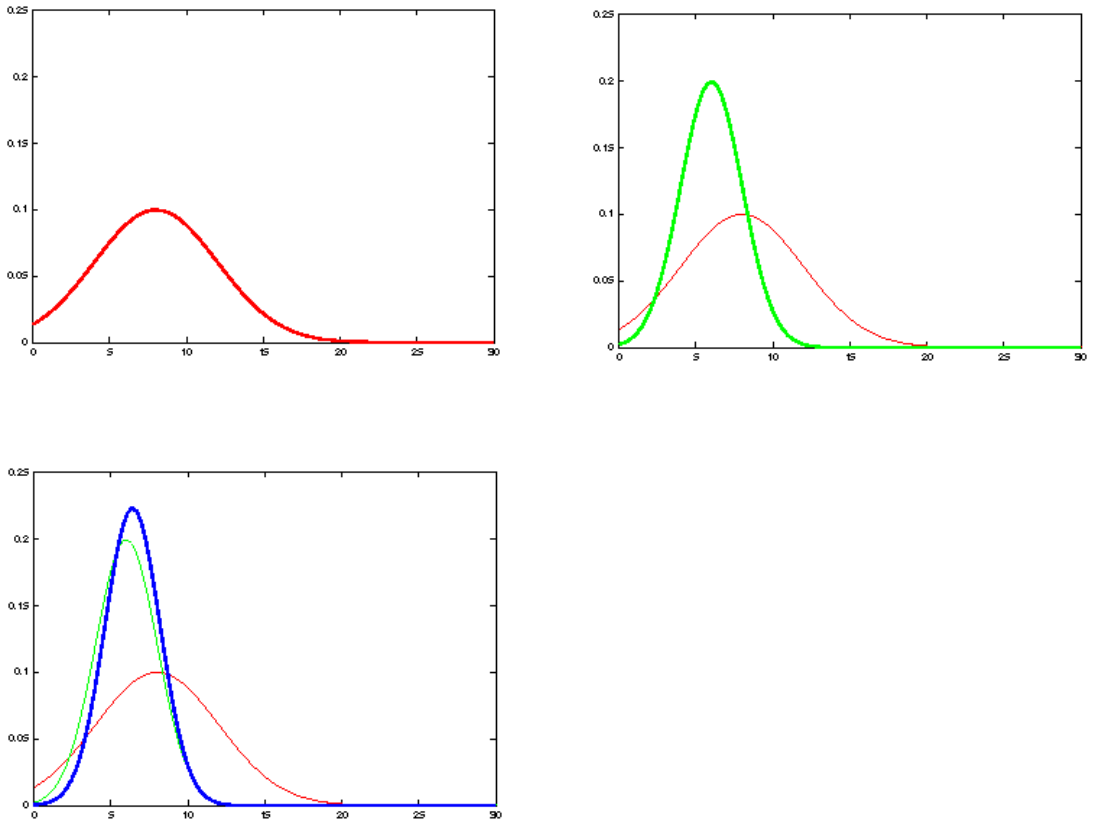

FIGURE 4.1: Probability distributions of a one-dimensional state in the basic Kalman filter [30]. The red line is the probability density function (pdf) of the previous belief, the green one is the predicted Gaussian pdf of the new state and the blue line is the pdf of the new belief.

Afterwards, the predicted mean and covariance are corrected depending on the likelihood of the observed measurements:

$$\begin{aligned} K_t &= \overline{\Sigma_t} C_t^T (C_t \overline{\Sigma_t} C_t^T + Q_t)^{-1} \\ \mu_t &= \overline{\mu_t} + K_t(\mathbf{z}_t - C_t \overline{\mu_t}) \\ \Sigma_t &= (I - K_t C_t)\overline{\Sigma_t} \end{aligned} \tag{4.9}$$

where Q_t is the covariance matrix of the measurement noise. The two steps of the Kalman filter in a case of a one-dimensional state can be seen in Fig. 4.1. Upper left the probability density function (pdf) of the previous state is shown. The result of using the Eq. 4.8 on it is the green function that can be seen on the upper right. Finally, lower left, the new pdf of the state estimated with the Eq. 4.9 is represented with the blue line.

In our case, the relationship between the state and the measurement is not linear and therefore can not be expressed as a matrix. It is governed by a non linear function h,

which is called the sensor model:

$$\vec{z}_t = h(\vec{x}_t) + \varphi_t \tag{4.10}$$

The state transition matrices can be also written as a function g, the so-called motion model:

$$\vec{x}_t = g(\mathbf{u}_t, \vec{x}_{t-1}) + \varepsilon_t \tag{4.11}$$

These functions need to be linearized, as the Kalman filter is based on the fact that a linear transformation of a Gaussian random variable results in another Gaussian random variable. The linearization can be done with the Taylor expansion (extended Kalman filter) or with the unscented transform (unscented Kalman filter). The extended Kalman filter (EKF) approximates a non linear function from its value at a certain point and its slope [31], which is the partial derivative in the case of a $\mathbf{x}_{t-1}$ vector of size one:

$$\begin{aligned} g'(\mathbf{u}_t, \mathbf{x}_{t-1}) &= \frac{\partial g(\mathbf{u}_t, \vec{x}_{t-1})}{\partial x_{t-1}} \\ g(\mathbf{u}_t, \mathbf{x}_{t-1}) &\approx g(\mathbf{u}_t, \mu_{t-1}) + g'(\mathbf{u}_t, \mathbf{x}_{t-1})(\mathbf{x}_{t-1} - \mu_{t-1}) \end{aligned} \tag{4.12}$$

The g function is evaluated at the mean μ_{t-1} due to the fact that the probability distributions are assumed to be Gaussian, therefore the most probable values are surrounding the mean. As the vector $\mathbf{x}_{t-1}$ is usually composed of more than one value and each value is associated to one or more g_i functions, the partial derivative must be replaced by the Jacobian matrix, which is defined as follows:

$$G_t = \begin{bmatrix} \frac{\partial g_1}{\partial x_1} & \frac{\partial g_1}{\partial x_2} & \cdots & \frac{\partial g_1}{\partial x_n} \\ \frac{\partial g_2}{\partial x_1} & \frac{\partial g_2}{\partial x_2} & \cdots & \frac{\partial g_2}{\partial x_n} \\ \vdots & \vdots & \cdots & \vdots \\ \frac{\partial g_m}{\partial x_1} & \frac{\partial g_m}{\partial x_2} & \cdots & \frac{\partial g_m}{\partial x_n} \end{bmatrix} \tag{4.13}$$

Replacing the Jacobian in the Eq. 4.12:

$$g(\mathbf{u}_t, \mathbf{x}_{t-1}) \approx g(\mathbf{u}_t, \mu_{t-1}) + G_t(\mathbf{x}_{t-1} - \mu_{t-1}) \tag{4.14}$$

The h function can be linearized in the same way with another Jacobian matrix H_t. As a whole, the EKF algorithm in pseudocode is presented in Alg. 4.0.1.

Algorithm 4.0.1: EXTENDEDKALMANFILTER$(\mu_{t-1}, \Sigma_{t-1}, \mathbf{u}_t, \mathbf{z})$

$\overline{\mu_t} = g(\mathbf{u}_t, \mu_{t-1})$
$\overline{\Sigma_t} = G_t \Sigma_{t-1} G_t^T + R_t$
$K_t = \overline{\Sigma_t} H_t^T (H_t \overline{\Sigma_t} H_t^T + Q_t)^{-1}$
$\mu_t = \overline{\mu_t} + K_t(\mathbf{z}_t - h(\overline{\mu_t}))$
$\Sigma_t = (I - K_t H_t)\overline{\Sigma_t}$
return (μ_t, Σ_t)

Calculating the Jacobian matrices lead to a high computational effort. Due to this fact, the unscented Kalman filter is implemented, which is cheaper in computation. The next sections describe the motion and sensor models and the linearization with the unscented transform.

Motion Model

The design of the motion model is crucial for the proper estimation of the state transition, and therefore for efficiency and accuracy of the localization. The motion model is based on the model in [3]. In the model, we assume that no control over the movement of the receiver is given, hence the control command represents just the time which has passed since the last computation. For the movement, and therefore the next estimated position of the receiver, we use a constant velocity model. This model assumes that the receiver moves with constant velocity, while changes in the velocity are undetermined, which is modeled by Gaussian noise with a covariance matrix Σ_V. In this model, the position and velocity of the receiver are updated according to the Euler integration scheme by

$$\begin{aligned} \mathbf{M}_{t+1} &= \mathbf{M}_t + h_t \mathbf{V}_t \\ \mathbf{V}_{t+1} &= \mathbf{V}_t + \zeta_t \,, \qquad \zeta_t \sim \mathcal{N}(0, \Sigma_V) \end{aligned} \tag{4.15}$$

where $h_t = T_{k_i i} - T_{k_j j} > 0$ is the time between the current signal from sender i and the previous signal from sender j. In order to calculate the offset between $\mathbf{S}_i$ and $\mathbf{S}_j$ with respect to the sending times t_{0i}, t_{0j} this equation is used

$$\delta_{ij} = (k_i I_i + t_{0i}) - (k_j I_j + t_{0j}) + \mathcal{N}(x; \mu, \sigma^2) \tag{4.16}$$

where $\mathcal{N}(x; \mu, \sigma^2)$ is normal distributed with mean μ and variance σ^2 As the offsets are transitive, we settle to estimate $m - 1$ offsets. Without loss of generality we estimate only the offset relative to sender $j = 1$ and define $\delta_i = \delta_{1i}$, where $\delta_1 = 0$.

Also the sending time of one sender must be estimated, as in TDOA only relative distances are measured. To propagate the estimated sending time of the latest received signal of sender i we use the last estimated sending time, the interval length and a normal distributed noise term as

$$t_{k_i i} = t_{(k_i-1)i} + I_i + \mathcal{N}(x; \mu, \sigma^2) \; . \tag{4.17}$$

We add the normal distributed noise $\mathcal{N}$ to increase the variance of the estimated offsets. As the send times $t_{k_i i}$ are all relative we estimate only $t_{k_1 1}$.

Sensor Models

The sensor models use the measurement, which in this case is the timestamp of the received signal, to correct the state transition estimated by the motion model. There are two different sensor models, one for the TDOA and another for the FDOA. The TDOA sensor model predicts the measurement with the current state and the wave propagation velocity:

$$\overline{z}_t = \frac{1}{c}\|\mathbf{M}_t - \mathbf{S}_j\| + (t_{k_1 1} + \delta_j) \tag{4.18}$$

where $\overline{z}_t$ is the predicted measurement. The FDOA sensor model is calculated taking into account also the previous measurement of the same sender and the estimated state when it was received:

$$\overline{z}_t = \frac{1}{c}(\|\mathbf{M}_{t,j} - \mathbf{S}_j\| - \|\mathbf{M}_{t-1,j} - \mathbf{S}_j\|) + I_j + z_{t-1,j} \tag{4.19}$$

where $\mathbf{M}_{t-1,j}$ is the estimated position of the receiver when the previous measurement of the sender j was received. This measurement is noted as $z_{t-1,j}$.

Unscented Kalman Filter

The unscented Kalman filter (UKF), which was proposed by Julier and Uhlman [32], is a recursive state estimator based on the unscented transform [31, 33], an approach to linearization of non-linear models. For a random variable with dimension L, $2L + 1$ “sigma

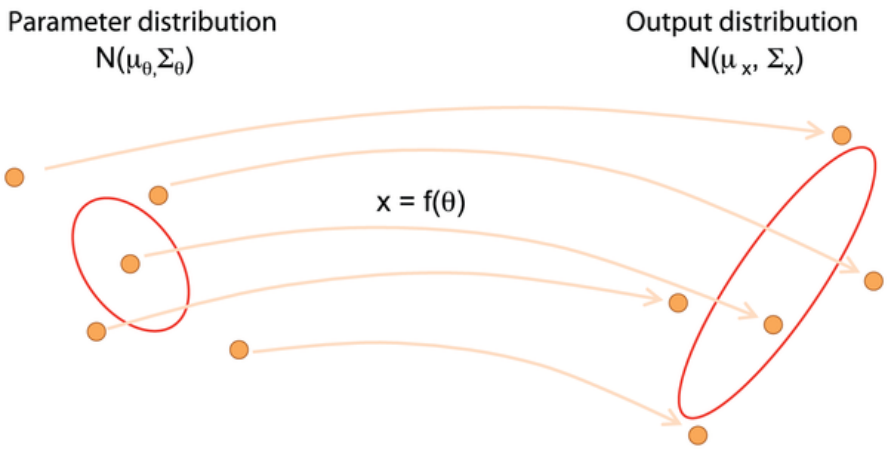

FIGURE 4.2: Schematic representation of the unscented transformation [34], where $\mu_\bullet$ is the mean and $\Sigma_\bullet$ is the covariance matrix.

points" are generated deterministically with the known covariance matrix of the involved variables and the tuning parameters of the filter. Afterwards each point is passed through the non linear function creating a cloud of transformed points, which are weighted and used to compute their Gaussian statistics. A schematic representation of this is shown in Fig. 4.2. As the evaluation of the models is calculated only for the $2L+1$ sigma points, the UKF is cheaper in computation than the extended Kalman filter, which requires calculation of the Jacobian matrix, or the particle filter, which requires evaluation of a large number of particles. For the implementation of the UKF for tracking of a moving receiver by unsynchronized TDOA the description given in [31] is followed.

Unscented Kalman Filter using only TDOA or FDOA Measurements

Generating sigma points

First, an extended mean vector and covariance matrix are generated:

$$\begin{aligned} \mu_{t-1}^{a} &= \begin{pmatrix} \mu_{t-1}^{T} & \mu_{V}^{T} & \mu_{m}^{T} & \mu_{o}^{T} \end{pmatrix}^{T} \\ \Sigma_{t-1}^{a} &= \begin{bmatrix} \Sigma_{t-1} & 0 & 0 & 0 \\ 0 & \Sigma_{V} & 0 & 0 \\ 0 & 0 & \sigma_{m}^{2} & 0 \\ 0 & 0 & 0 & \Sigma_{o} \end{bmatrix} \end{aligned} \tag{4.20}$$

where Σ_o is the covariance matrix of the offset noise, σ_m^2 is the variance of the measurement noise and μ_{t-1}, μ_V, μ_m, μ_o are the mean of the previous state, the velocity noise, the measurement noise and the offset noise, respectively. The velocity and the offset noise are called "process noise".

The augmented mean and variance are used to generate a set of $2L$ sigma points, where L is the dimension of the augmented mean vector:

$$\chi^a_{t-1} = \begin{bmatrix} \mu^{a\,T}_{t-1} \\ \left(\mu^a_{t-1} + \sqrt{(L+\lambda)\Sigma^a_{t-1,[1]}}\right)^T \\ \vdots \\ \left(\mu^a_{t-1} + \sqrt{(L+\lambda)\Sigma^a_{t-1,[L]}}\right)^T \\ \left(\mu^a_{t-1} - \sqrt{(L+\lambda)\Sigma^a_{t-1,[1]}}\right)^T \\ \vdots \\ \left(\mu^a_{t-1} - \sqrt{(L+\lambda)\Sigma^a_{t-1,[L]}}\right)^T \end{bmatrix}^T , \tag{4.21}$$

where $\Sigma^a_{\bullet,[\ell]}$ denotes the ℓ-th column of $\Sigma^a_\bullet$. The scaling parameter

$$\lambda = \alpha^2(L+\rho) - L \tag{4.22}$$

determines how far the sigma points are from the mean, where α and ρ are tuning parameters of the filter.

Prediction

The sigma points matrix has now a dimension of $L \times (2L+1)$. This matrix has rows in the space of the previous state, the measurement noise and the process noise:

$$\chi^a_{t-1} = \begin{bmatrix} \chi^x_{t-1} & \chi^m_t & \chi^o_t & \chi^V_t \end{bmatrix}^T \tag{4.23}$$

Each row has $2L+1$ sigma points. The sigma points of the previous state and the process noise are passed to a function g, which is the motion model defined in Eqns. (4.16) and (4.15), to predict the new state:

$$\chi^x_t = g(u_t, \chi^x_{t-1}, \chi^V_t, \chi^o_t) \tag{4.24}$$

After that, the Gaussian statistics of the new points are computed by

$$\overline{\mu}_t = \sum_{l=0}^{2L} w_m(l)\chi^x_{l,t} , \qquad \overline{\Sigma}_t = \sum_{l=0}^{2L} w_c(l)\chi^x_{l,t} , \tag{4.25}$$

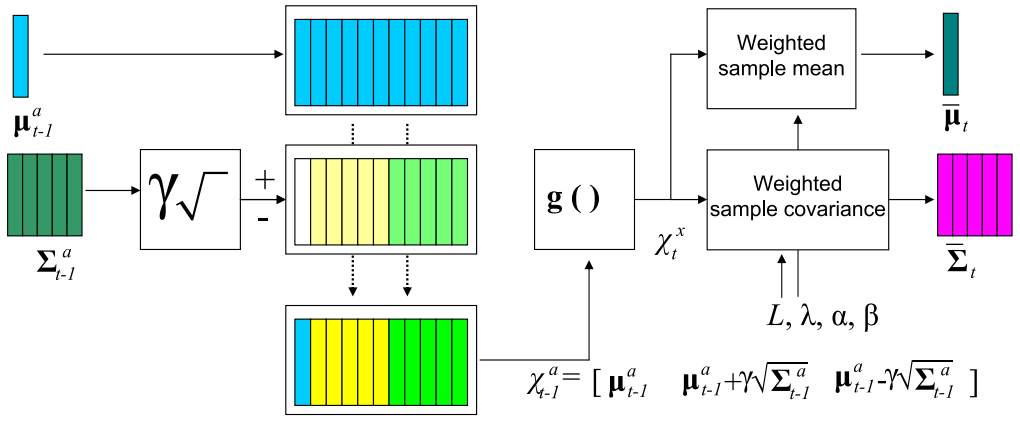

FIGURE 4.3: Schematic diagram of the unscented transformation [35], where $\gamma = \sqrt{L + \lambda}$.

where

$$
\begin{aligned}
w_m(0) &= \frac{\lambda}{L+\lambda} \\
w_c(0) &= \frac{\lambda}{L+\lambda} + (1 - \alpha^2 + \beta) \\
w_m(l) = w_c(l) &= \frac{1}{2(L+\lambda)} \, . \qquad\qquad (1 \leq l \leq 2L)
\end{aligned}
$$

The parameter β is a tuning parameter of the filter which has to be set depending on the a priori knowledge of the state probability distribution. A schematic diagram of all the transformation explained above is shown in Fig. 4.3.

The observations at the sigma points are calculated in the sensor model by

$$\overline{z}_t = h(\chi_t^x) + \chi_t^m \, . \tag{4.26}$$

where h can be either the sensor model defined in Eq. (4.18) or Eq. (4.19) depending which method is used.

Correction

In the final step, the Gaussian statistics of the observations at the sigma points and the predicted state are calculated to correct the measurement.

$$\begin{aligned} \mu_{t,z} &= \sum_{l=0}^{2L} w_m(l)\, \overline{z}_{l,t} \\ \sigma_z^2 &= \sum_{l=0}^{2L} w_c(l)\, (\overline{z}_{l,t} - \mu_{t,z})^2 \end{aligned} \tag{4.27}$$

In this step also the cross-covariance between the predicted state and the predicted measurement is calculated:

$$\Sigma^{x,z} = \sum_{l=0}^{2L} w_c(l)\, (\overline{\chi}_{l,t}^x - \overline{\mu}_t)\, (\overline{z}_{l,t} - \mu_{t,z})^T \tag{4.28}$$

Finally, the mean and the covariance of the state are updated by

$$\begin{aligned} \mu_t &= \overline{\mu}_t + K_t(z - \mu_z) \\ \Sigma_t &= \overline{\Sigma}_t - K_t K_t^T \sigma_z^2 \,, \end{aligned} \tag{4.29}$$

where $K_t = \frac{1}{\sigma_z^2}\, \Sigma^{x,z}$ is the Kalman gain.

Unscented Kalman Filter using TDOA and FDOA Measurements

To minimize the error, a good strategy is to take into account the TDOA and the FDOA measurements.

As two sensor models are used at the same time, there have to be two different noises, one for each sensor model. This means there is a new component in the extended mean and covariance:

$$\begin{aligned} \mu_{t-1}^a &= \begin{pmatrix} \mu_{t-1}^T & \mu_V^T & \mu_{m_{FD}}^T & \mu_{m_{TD}}^T & \mu_o^T \end{pmatrix}^T \\ \Sigma_{t-1}^a &= \begin{bmatrix} \Sigma_{t-1} & 0 & 0 & 0 & 0 \\ 0 & \Sigma_V & 0 & 0 & 0 \\ 0 & 0 & \sigma_{m_{FD}} & 0 & 0 \\ 0 & 0 & 0 & \sigma_{m_{TD}}^2 & 0 \\ 0 & 0 & 0 & 0 & \Sigma_o \end{bmatrix} \end{aligned} \tag{4.30}$$

where $\mu^T_{m_{FD}}$ and $\mu^T_{m_{TD}}$ are the mean of the measurement noise of the FDOA and TDOA respectively. The variances of them are represented as $\sigma^2_{m_{FD}}$ and $\sigma^2_{m_{TD}}$.

The sigma points are generated as in Eq. (4.21) and the resultant matrix has now components of the two measurement noises:

$$\chi^a_{t-1} = \begin{bmatrix} \chi^x_{t-1} & \chi^{m_{FD}}_t & \chi^{m_{TD}}_t & \chi^o_t & \chi^V_t \end{bmatrix}^T \tag{4.31}$$

The prediction step remains the same until the sensor model is used, as the motion model has not been changed. When the observations at the sigma points are calculated, the dimension of the measurement vector and its noise are set to two instead of one for every sigma point:

$$\overline{z}_t = \begin{bmatrix} h_{TDOA}(\chi^x_t) \\ h_{FDOA}(\chi^x_t) \end{bmatrix} + \begin{bmatrix} \chi^{m_{TD}}_t \\ \chi^{m_{FD}}_t \end{bmatrix} \tag{4.32}$$

The mean of the predicted measurement is now a vector of two dimensions and its covariance is a matrix of 2×2:

$$\mu_{t,z} = \sum_{l=0}^{2L} w_m(l)\, \overline{z}_{l,t} \qquad \Sigma_{zz} = \sum_{l=0}^{2L} w_c(l)\, (\overline{z}_{l,t} - \mu_{t,z})(\overline{z}_{l,t} - \mu_{t,z})^T \tag{4.33}$$

The mean of the predicted measurement is used to calculate its cross-covariance with the predicted state:

$$\Sigma^{x,z} = \sum_{l=0}^{2L} w_c(l)\, (\overline{\chi}^x_{l,t} - \overline{\mu}_t)\, (\overline{z}_{l,t} - \mu_{t,z})^T \tag{4.34}$$

As now the covariance of the measurement is a matrix and not a scalar, the Kalman gain K is not calculated with its reciprocal but with its inverse:

$$K_t = \Sigma^{x,z}\, \Sigma^{-1}_{zz} \tag{4.35}$$

Finally, the mean and the covariance of the state are updated also taking into account the new dimension of the measurement:

$$\mu_t = \overline{\mu}_t + K_t(z - \mu_z) \qquad \Sigma_t = \overline{\Sigma}_t - K_t \Sigma_{zz} K_t^T \ ,$$

Chapter 5

Evaluation and Discussion

Simulation

The simulations and the UKF algorithm have been implemented in Matlab. To calculate the real timestamps the desired trajectory is polygonized. A set of points of the trajectory are passed to the simulation algorithm and they are connected with lines. Once this lines are generated, the intersections between the lines and the sent signals are calculated with a simple system of equations. For each line:

$$\begin{cases} \frac{1}{c}\|\mathbf{M} - \mathbf{S}_i\| + t_{k_i i} = t \\ \mathbf{M}_0 + \mathbf{v}(t - t_0) = \mathbf{M} \end{cases} \tag{5.1}$$

where $\mathbf{M}_0$ and t_0 are the initial position and time of the receiver in the line. As in the simulations the velocity is assumed to be fixed with a constant v_c during all the trajectory, the velocity vector $\mathbf{v}$ is calculated as follows:

$$\mathbf{v} = \left(\frac{(\mathbf{M}_f - \mathbf{M}_0)}{\|\mathbf{M}_f - \mathbf{M}_0\|} \right) v_c \tag{5.2}$$

where M_f is the initial point of the next line. The system of equations intersect in two points, a point in the past, which is dismissed, and a candidate to be the real timestamp: Γ. The position of the receiver at Γ is calculated and compared with $\mathbf{M}_f$ to ensure it pertains to the current line. If it does not, the equation of the next line is

used until the real timestamp $T_{k_i i}$ is found. This procedure is described in Alg. 5.0.2.

Algorithm 5.0.2: FINDRECEIVEDTIMESTAMPS()

$find\ \Gamma$
while $\mathbf{v}\Gamma > \mathbf{M}_f$
do $\begin{cases} \mathbf{v} = next\ line\ velocity \\ \mathbf{M}_f = next\ line\ ending\ point \\ find\ \Gamma\ of\ the\ next\ line \end{cases}$
return (Γ)

To simulate a real scenario, a Gaussian distributed error variable $\xi \sim \mathcal{N}(0, \sigma_\xi^2)$ is added to each timestamp. In the experiments in [3] an ultrasound system was used, where a standard deviation of approximately 0.1 ms was a typical magnitude of error. In these simulations a slightly larger timing noise of $\sigma_\xi = 0.3$ ms is used in order to consider errors due to adverse environment settings, ensuring the robustness of the presented algorithm.

All of the experiments in 2D have been done with a fixed trajectory of the receiver, moving in an experiment area of 15 m × 15 m with a velocity of 0.4 m/s. The same applies to the 3D experiments, but the receiver changes also its altitude and the experiment area has a size of 15 m × 15 m × 15 m as it is a 3D scenario.

To calculate the mean error and standard deviation of the error of one simulation, for each measurement the distance between the true position and the position estimated is calculated by

$$\begin{aligned} \mu_\varepsilon &= \frac{1}{n}\sum_{t=1}^{n} \|\mathbf{M}_t - \overline{\mathbf{M}}_t\| \\ \sigma_\varepsilon^2 &= \frac{1}{n-1}\sum_{t=1}^{n} \left(\|\mathbf{M}_t - \overline{\mathbf{M}}_t\| - \mu_\varepsilon\right)^2 , \end{aligned} \tag{5.3}$$

where $\mathbf{M}_t$ represents the true position and $\overline{\mathbf{M}}_t$ the estimated position at the arrival of the t-th signal, and n is the total number of received signals in one simulation.

The experiments were executed assuming that the initial position and velocity of the receiver are known, and the process noise variance is:

$$\Sigma_V = \begin{pmatrix} \sigma_V^2 & 0 \\ 0 & \sigma_V^2 \end{pmatrix} \tag{5.4}$$

TABLE 5.1: Sender positions and interval lengths for the senders used in 2D.

	$\mathbf{S}_1$	$\mathbf{S}_2$	$\mathbf{S}_3$
Position x (m)	4	15	0
Position y (m)	0	11	15
Interval (s)	0.031	0.041	0.047

TDOA

Employment of the Kalman filter requires good knowledge of the process noise variance and the measurement noise variance. The Kalman parameters are dependent on the parameters of the simulation, which are the velocity and trajectory of the receiver, the distribution of measurement error, and the senders positions and signal intervals. For this first experiment, only the TDOA measurements were used and the senders and the receivers were located in 2 dimensions.

The senders were located at remote positions of the field (Table 5.1), to reduce the effect of adverse sender positioning.

We ran an experiment of the UKF variating both parameters, while adding the Gaussian error to the true measurements. The results in Fig. 5.1 indicate that localization precision decreases slightly if the process noise variance is overestimated, however the UKF becomes unstable if process noise is underestimated, as the receiver estimate cannot follow the curvy trajectory. Now, the experiment was repeated 100 times, fixing the measurement noise variance to $\sigma_m^2 = 31.626\,\mathrm{ms}^2$, for each magnitude of the process noise variance. The result is shown in Fig. 5.2. The same experiment but fixing the process variance to $\sigma_V^2 = 0.025\,\mathrm{m}^2/\mathrm{s}^2$ is shown in Fig. 5.3.

When the parameters are properly adjusted, the mean error is reduced to 0.068 m with a standard deviation of 0.042 m.

FDOA

Using only the FDOA measurements lead to much bigger errors. When the parameters are properly adjusted, the mean error is 0.400 m with a standard deviation of 0.197 m. This is because one of the assumptions made in the probabilistic state estimation was that the measurement does not depend on the previous states and measurements, which is not true in the case of the FDOA. Furthermore, as two timestamps are used it is more affected by the noise. Nevertheless, using it in combination with the TDOA can reduce the error, as proved in the next section.

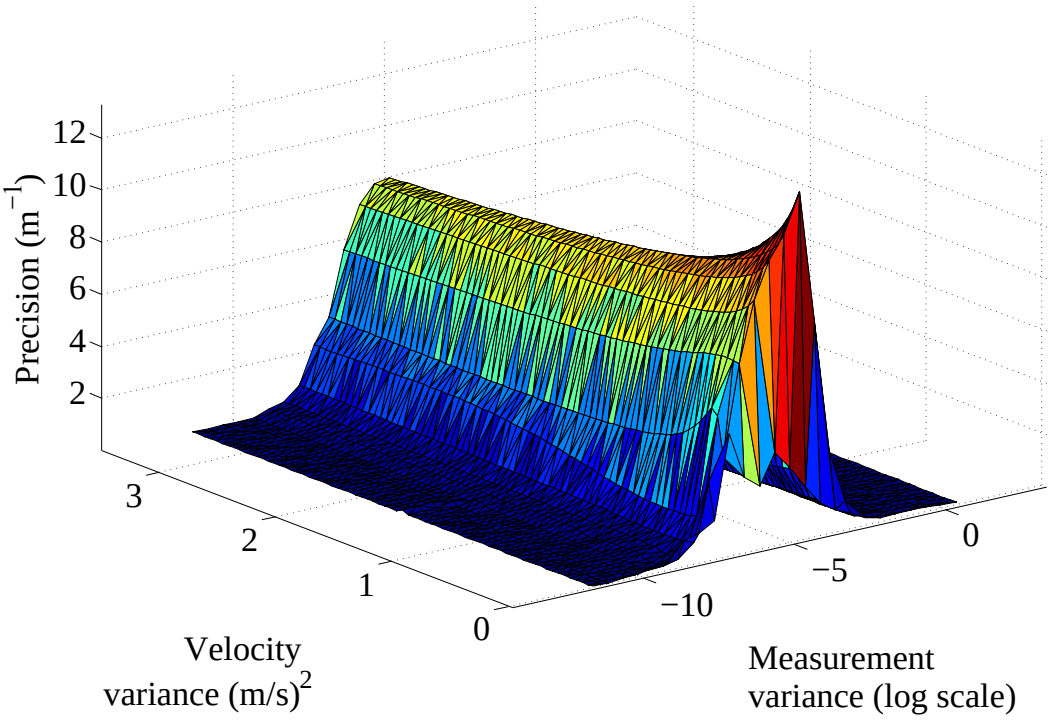

FIGURE 5.1: Inverse of the UKF mean error with respect to different parameter settings of process noise variance and measurement noise variance. The measurement variance is represented on a log scale by $\log_{10}(\sigma_m^2)$. Good knowledge of the process and measurement errors increases the precision of receiver localization immensely.

TDOA and FDOA

The combination of the TDOA and the FDOA is a good strategy to reduce the error, this is reduced to 0.051 m with a standard deviation of 0.027 m. The main disadvantage is that a new parameter has to be set, the performance of the algorithm depends now on the correct adjustment of the process error and the measurement error of the TDOA and the FDOA.

To note the benefits of using this combination, the same simulation is done with the three algorithms as shown in Fig. 5.4. In Fig. 5.5 can be seen the error of each strategy for every received signal. The TDOA has a mean error of 0.067 m and a standard deviation of 0.041 m. The combination of the TDOA and the FDOA has a mean error of 0.047 m and a standard deviation of 0.026 m. The error of the FDOA is much higher than the others, it has a mean error of 0.274 m and a standard deviation of 0.132 m. In the figure 5.6 the cumulative distribution functions of these simulations are represented.

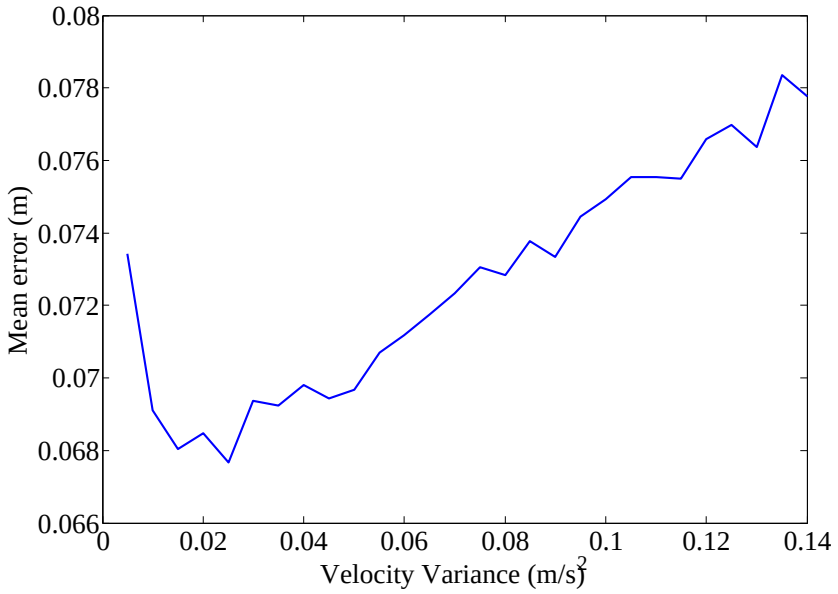

FIGURE 5.2: Fixed measurement noise variance $\sigma_m^2 = 31.626\,\mathrm{ms}^2$ with TDOA in a 2D scenario. If the process variance is fixed between $0.005\,\mathrm{m}^2/\mathrm{s}^2$ and $0.14\,\mathrm{m}^2/\mathrm{s}^2$ the mean localization error is below 0.079 m.

TABLE 5.2: Sender positions and interval lengths for the senders used in 3D.

	$\mathbf{S}_1$	$\mathbf{S}_2$	$\mathbf{S}_3$	$\mathbf{S}_4$
Position x (m)	15	0	0	15
Position y (m)	0	0	15	15
Position z (m)	0	15	0	15
Interval (s)	0.031	0.041	0.047	0.053

3 Dimensions

The combination of TDOA and FDOA can be extended to three dimensions just increasing the dimension of $\mathbf{M}_t$, $\mathbf{S}_i$ and $\mathbf{V}_t$ to three. As explained in section 3 to estimate a position in three dimensions is mandatory to have at least 4 senders. These senders are located in four corners of the field (Table 5.2). Fig. 5.7 shows the real position and the estimated position by the algorithm. The mean error of the algorithm calculated running 100 times this simulation is 0.141 m with a standard deviation of 0.036. The error is highly increased as one additional variable has to be estimated and the trajectory is highly bended in the three dimensions.

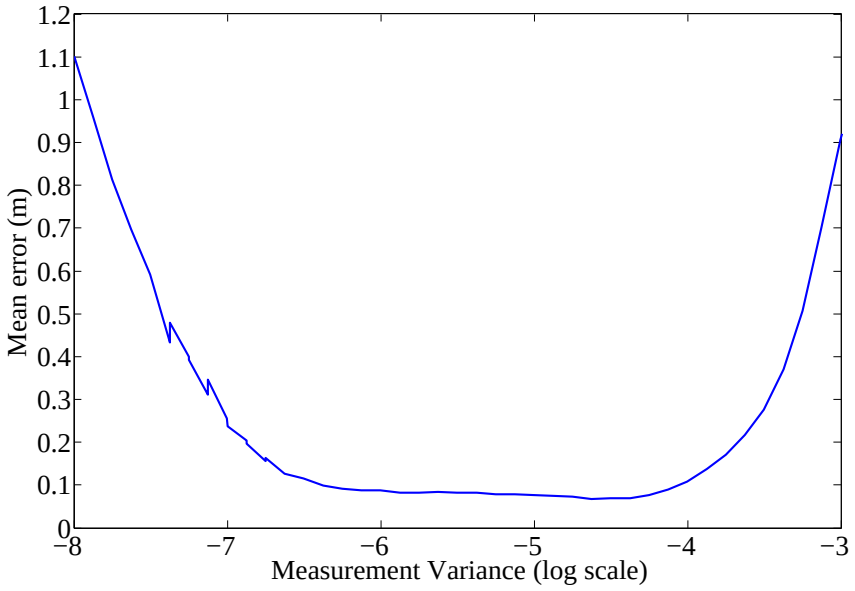

FIGURE 5.3: Fixed process variance $\sigma_V^2 = 0.025\,\mathrm{m}^2/\mathrm{s}^2$ with TDOA in a 2D scenario. If the measurement variance is fixed between $0.75\,\mathrm{ms}^2$ and $75\,\mathrm{ms}^2$ the mean localization error is below 0.090 m. The measurement variance is represented on a log scale by $\log_{10}(\sigma_m^2)$.

Senders in 3D and Receiver in 2D

One could think of an scenario where a robot is moving on the floor. In this situation, there is no need to estimate its altitude but the senders can be placed in three dimensions. To do this simulation the senders are located in the same positions than in 2D (Table 5.1) but with an altitude of 15 m, 7.5 m and 0 m for the senders 1, 2 and 3 respectively. Using the TDOA and the FDOA measurements and with the parameters properly adjusted the mean error achieved is 0.077 m with a standard deviation of 0.048 m. The error is higher than in 2D as the senders are farther from the receiver. The next simulations are done with the senders in 3D and the receiver in 2D, as it is a realistic scenario and the computation time is lower than in 3D.

Influence of the Temperature in the Error

The ultrasound velocity is assumed to be 343 m/s in the algorithm, but this is only true at 20°C with dry air. The humidity has been proved to have a limited effect on the ultrasound velocity. In [36] has been demonstrated that changing the humidity from 0% to 100% with a temperature of 20°C increases the velocity only a 0.375%.

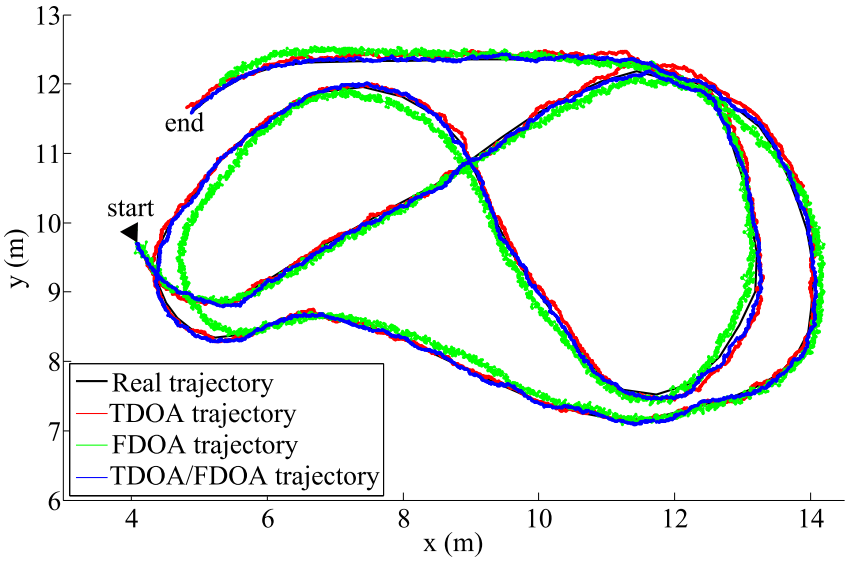

FIGURE 5.4: Real and estimated positions using TDOA, FDOA and combinating the FDOA and the TDOA. The bigger errors are in the curves due to the constant velocity motion model.

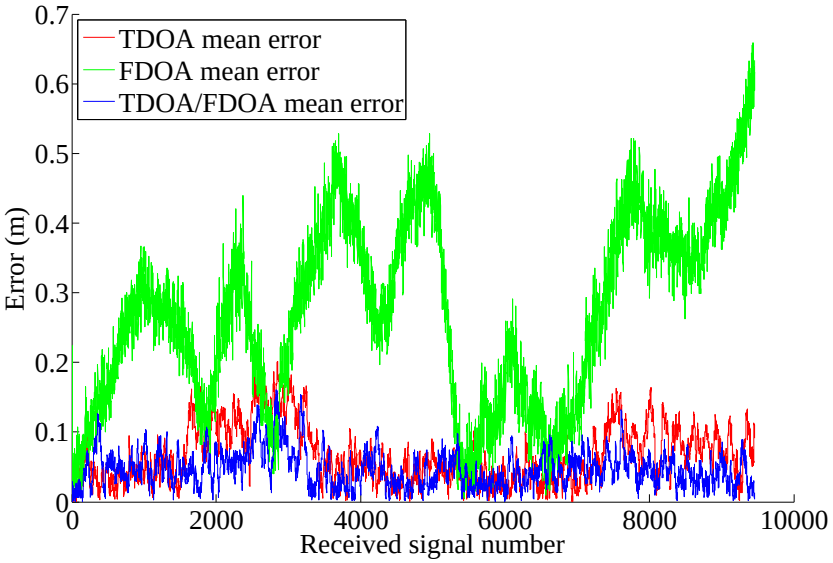

FIGURE 5.5: Mean error of the execution in Fig. 5.4

The ultrasound velocity dependence on the atmospheric pressure for an ideal gas can be written as:

$$c(T) = \sqrt{\frac{\gamma P}{\rho}} \tag{5.5}$$

where P is the static atmospheric pressure, γ is the heat capacity ratio (is 1.4 for dry

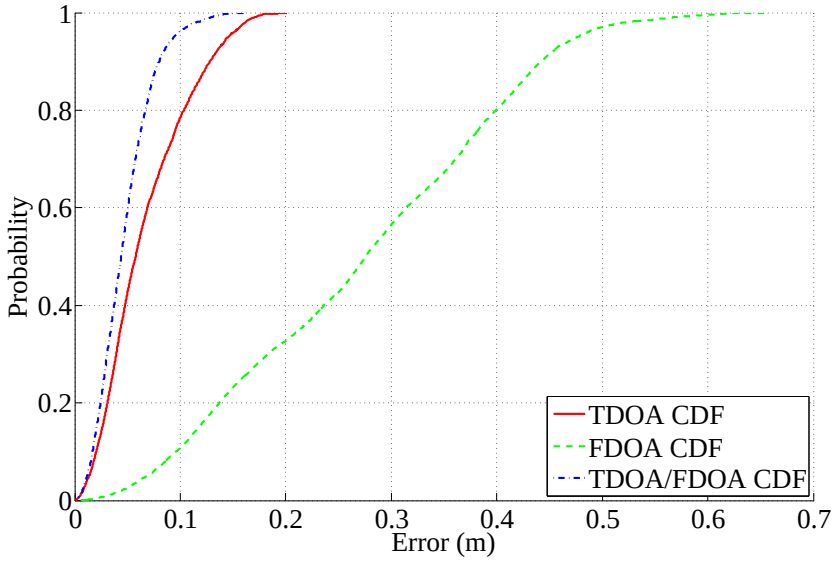

FIGURE 5.6: Cumulative distribution functions of the receiver error for one execution in 2D. It can be seen that the combination of the TDOA and FDOA has a moderate advantage over the TDOA and a huge advantage over the FDOA.

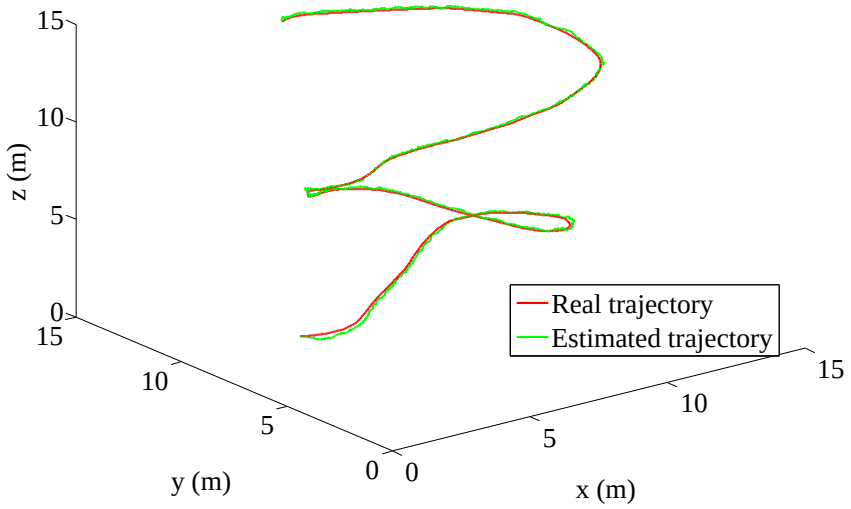

FIGURE 5.7: Real and estimated positions in 3D using the TDOA and the FDOA measurements.

air) and ρ the density of the gas. As if the pressure increases also does the density, the ultrasound velocity is not affected by the pressure. The air can be considered as an ideal gas [37], with $\frac{\gamma P}{\rho} = RT$ where R is the thermodynamic constant characteristic of the gas (287 N· m/(Kg K) for air), M is the molar mass (the mean molar mass for dry air is about 0.0289645 kg/mol) and T the absolute temperature in Kelvin. Therefore the temperature can highly increase the error if the temperature differs greatly from 20°C.

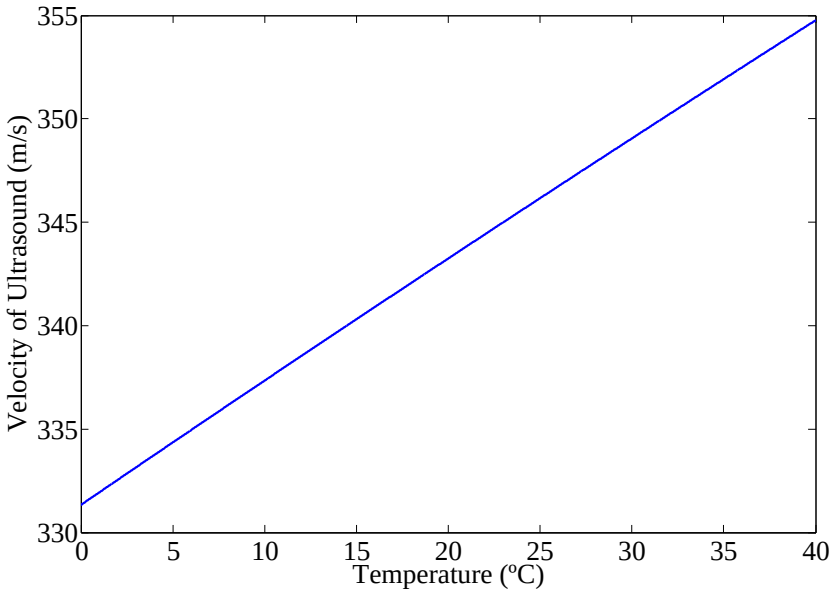

FIGURE 5.8: Effect of the temperature on the ultrasound velocity.

This is because the molecules vibrate faster if the temperature is increased, as they have more energy. The dependence is shown in Fig. 5.8 and can be written as:

$$c(T) = \sqrt{\frac{\gamma RT}{M}} \tag{5.6}$$

The effect of the temperature on the error can be seen in Fig. 5.10 and Fig. 5.9, where 100 simulations have been done for each value of the temperature. In Fig. 5.9 the parameters of the simulation are the same than in the last section. The minimum error is shifted to 24° instead of 20° due to the fact that the temperature has a high effect on the first estimated states by the filter and this distorts the mean of the entire simulation. This is proved in Fig. 5.10, where the values of the initial covariance matrix of the state are reduced to reflect complete knowledge of the initial position, velocity and offsets. This reduces the error, as in our case they are exactly known, but in a realistic scenario overestimating the knowledge of the initial values can lead to huge errors.

With low values in the covariance matrix the error at 20° is almost the same than at 22°, nonetheless the standard deviation is higher at 22°. The lowest temperatures have more effect on the error than the highest ones, as the algorithm is more unstable when the signals are delayed. The mean error at 0 ° is 0.237 m, with a standard deviation of 0.098 m. Nevertheless, at 40°, which distance from the mean also 20° , the mean error is 0.204 m with a standard deviation of 0.079 m. The covariance matrix of the estimated state by the UKF (Σ_t) is also affected by the temperature. The components of the estimated position are extracted from the main covariance matrix to see the effect of

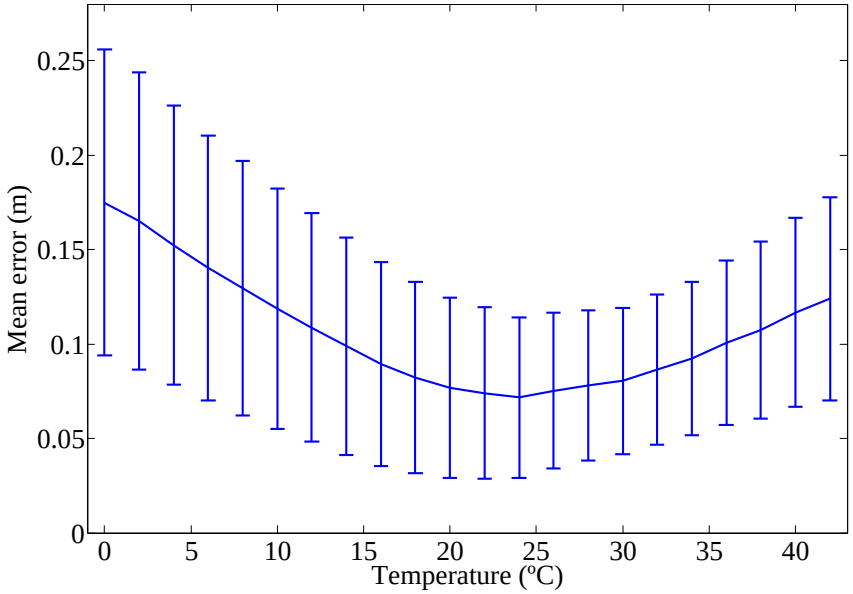

FIGURE 5.9: Effect of the temperature on the mean error for high values in the initial covariance matrix of the state. The vertical lines show the standard deviation. The senders are located in 3D and the receiver in 2D. The minimum error is achieved when the temperature is near the assumed one (20°C). If the temperature is between 14°C and 36°C the mean error is lower than 0.100 m

the temperature on them:

$$\Sigma_{t,xy} = \begin{pmatrix} \sigma_x^2 & \sigma_{xy} \\ \sigma_{yx} & \sigma_y^2 \end{pmatrix} \tag{5.7}$$

The determinant of this matrix increases with the temperature, as is shown in Fig. 5.11. The temperature could be somehow estimated modelling this relation.

Influence of the Interval Length and the Number of Senders in the Error

The number of senders is an important factor, as adding senders can reduce the error but having too many senders can increase the computational effort and the cost. To evaluate this effect the senders are randomly placed among the 2D scenario with a uniform distribution. Their intervals are also random between 0.025 s and 0.055 s. The result can be seen in Fig. 5.12. To do these simulations the parameters of the UKF are fixed with the same values than in the previous sections, which are the best for three senders located at remote positions of the field. Due to this fact, the error of using three senders is highly increased in the graph, as they are in random locations and the error is underestimated. Even so, if the assumed variances of the errors were increased,

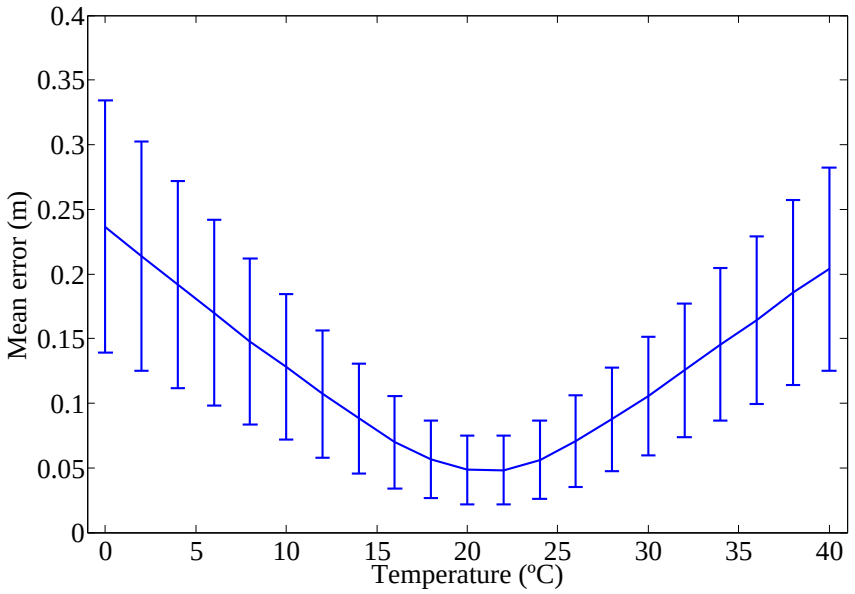

FIGURE 5.10: Effect of the temperature on the mean error for low values in the initial covariance matrix of the state. The vertical lines show the standard deviation. The senders are located in 3D and the receiver in 2D. The minimum standard deviation is achieved when the temperature is the assumed one (20°C). If the temperature is between 14°C and 28°C the mean error is lower than 0.090 m

the error would be overestimated for a huge number of senders and therefore the error increased. In conclusion, it is important to know approximately the number of senders that will be used to have a better performance of the filter.

The period of the signals plays also an important role in the performance of the UKF, as more received signals implies that the algorithm is executed more often and therefore more positions are estimated, reducing the error but increasing the computational effort. In Table. 5.3 the error when the intervals are multiplied by 10 and divided by 10 is shown. These experiments are also done with fixed parameters, this means that the error is underestimated when the intervals are multiplied by 10 and therefore the error is highly increased. A prove of this are the results in [19], where we obtained a mean error of 0.115 m with an interval of the same order of magnitude using only the TDOA measurements in a 2D scenario, but with the parameters properly adjusted. When the intervals are reduced the error is overestimated, nonetheless its performance is highly improved, as the number of received signals is multiplied by 10 and therefore also the estimated positions.

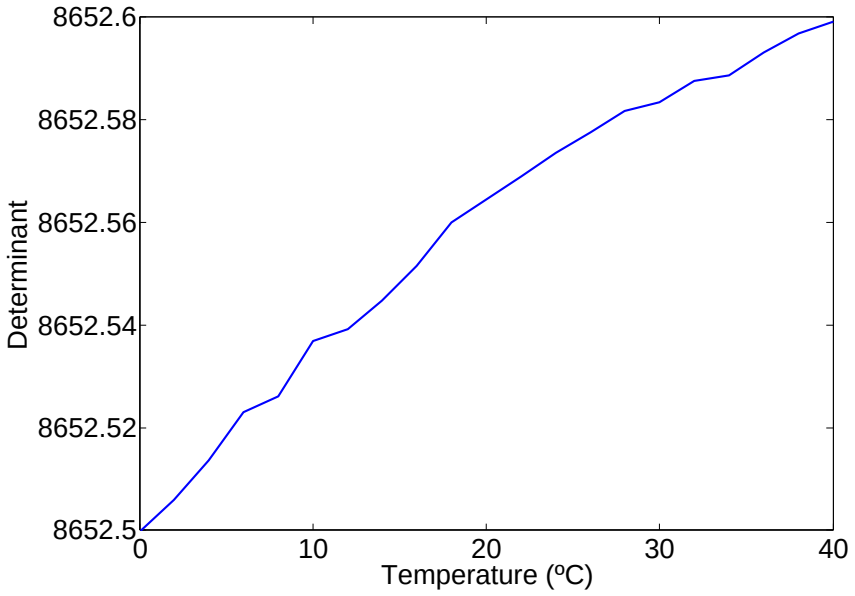

FIGURE 5.11: Effect of the temperature in the covariance of the estimated position. It can be seen that the determinant increases with the temperature.

TABLE 5.3: Mean error and standard deviation when the interval lengths are changed.

	$0.1I_i$	I_i	$10I_i$
Mean error (m)	0.060	0.077	0.223
Standard deviation (m)	0.034	0.048	0.140

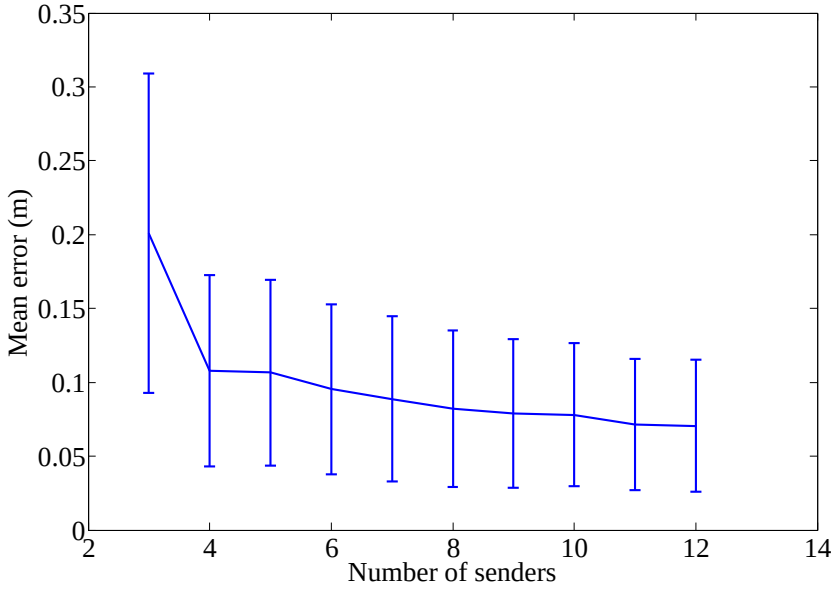

FIGURE 5.12: Effect of the number of senders on the mean error. The senders are located in random positions and with random intervals. The parameters of the filter are fixed.

Chapter 6

Conclusions and Perspectives

It has been shown that the unscented Kalman filter is capable to locate a moving receiver with the aid of unsynchronized senders regardless of the dimension of the space. Even so, the parameters of the filter have to be properly adjusted depending on the effect of the noise in the measurements. It has been proved that overestimating the noise effect has not as much impact on the error as underestimating it, which can lead to huge errors.

While using only the FDOA measurements has been demonstrated to highly increase the error, using them in combination with the TDOA measurements has been proved to be the best strategy to reduce the error. Nevertheless, using only the TDOA measurements is enough to precisely track the position of the receiver with a slightly higher error.

For the future work, it would be interesting to apply this algorithm in a real device. To do this, some challenges have to be overcome. Loss of signals could be a problem in a realistic scenario, specially due to the fact that the signals can collide. This would have a high effect on the FDOA measurements, where two consecutive timestamps of one sender are required. Furthermore, the parameters of the filter have to be set so that the receiver can move in a random trajectory without highly increase the error if the receiver stops suddenly or if it does an abrupt turn.

The initial position and velocity need to be estimated, as in this thesis they are assumed to be known beforehand. The UKF assumes Gaussian probabilities, which is not true in the case of the initial values. The initial position has a uniform probability among the map and the velocity may have a uniform probability as well with its limits depending on the robot or the person to track. As a uniform probability can be seen as a normal distribution with infinite covariance, one could estimate the initial values setting the initial covariance of the state with infinity along the main diagonal. Obviously this is

not possible in a real algorithm, but using high values instead can be a solution in some cases [38].

In our case the UKF has been proved to need a high number of received signals to achieve a reasonable error when the initial state is unknown, as can be seen in Fig. 6.1, where one simulation is done with the TDOA and FDOA measurements using three senders. The trajectory is created connecting 30 random points with a line in the experiment area. The initial mean values are set to zero and the values of the initial covariance matrix are set to 1000 in the case of the diagonal elements of the velocity and position, as using too large values can lead to huge rounding errors [39]. The variance of the offsets and t_{k1} are set to 0.001 resulting in an initial covariance matrix of the state as follows:

$$\Sigma_0 = \begin{bmatrix} 1000 & 0 & 0 & 0 & 0 & 0 & 0 \\ 0 & 1000 & 0 & 0 & 0 & 0 & 0 \\ 0 & 0 & 1000 & 0 & 0 & 0 & 0 \\ 0 & 0 & 0 & 1000 & 0 & 0 & 0 \\ 0 & 0 & 0 & 0 & 0.001 & 0 & 0 \\ 0 & 0 & 0 & 0 & 0 & 0.001 & 0 \\ 0 & 0 & 0 & 0 & 0 & 0 & 0.001 \end{bmatrix} \tag{6.1}$$

To avoid using high numbers some approaches estimate the inverse of the covariance matrix so that its elements can be set to zero (information filter). Nevertheless, it would increase the computational effort, as the UKF is faster in computation than the information filter when the size of the state vector is much higher than the measurement vector [40]. Using another algorithm like the particle filter for the initialization has been proved to be a good strategy [41] and would lead to better results, as the knowledge of the size of the room and the limit of the velocity could be used to estimate the initial values. Furthermore, the particle filter has been proved to be capable to locate the initial position of the receiver in this situation with the TDOA measurements [17].

The temperature has been proved to have an important effect on the error when it differs greatly from the assumed one. Using a thermometer is a solution, but it would increase the cost. It could be somehow estimated with the determinant of the covariance matrix of the state, modelling it as a function of the temperature. In the Fig. 5.11 the determinant increases faster in the lowest temperatures than in the highest ones, while it changes 0.065 from 0°C to 20°C it changes only 0.035 from 20°C to 40°C. therefore one could estimate the temperature doing various simulations changing the assumed

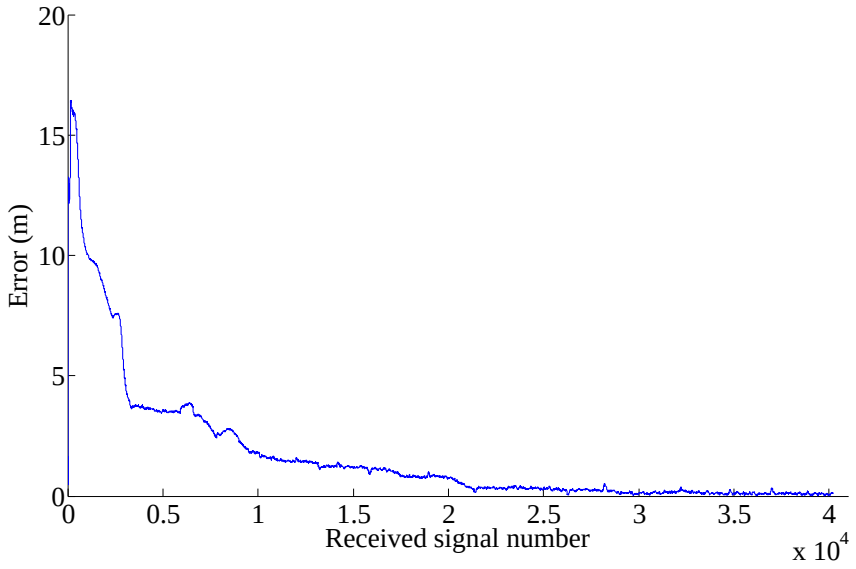

FIGURE 6.1: Error of the UKF when the initial position and velocity are unknown and a random trajectory is tracked. It achieves an error lower than 0.200 m only when 21350 signals are received, which is equivalent to more than 11 minutes in this case.

temperature and observing the variation of the determinant. Another alternative would be to use a root-finding algorithm like in [42], where the TDOA measurements of a set of receivers are used to estimate the speed of sound to precisely track the position of a sender. In the case proposed in this thesis the receiver has to be fixed to use a root-finding algorithm, as it needs a closed-form expression. An interesting improvement may be that the receiver takes profit of the measurements while it is not moving to correct the ultrasound velocity. As if the receiver is not moving the signals of the sender i are ideally received every I_i seconds, a threshold may be set to find out that the receiver is not moving and therefore the ultrasound velocity can be estimated.

Sending signals with an exact fixed interval during a large period of time is not possible with real clocks. The drift depends on the quality of the clock used [43]. While ordinary clocks drift by around 1 μs, the high precision quarz clock drift rate is approximately 10 or 100 ns/s. As it is a cumulative error it can not be neglected. A cumulative error has a critical effect on this approach, as if the error changes excessively the parameters have to be changed. Furthermore, after a long period of time the error would highly deteriorate the performance of the filter. After one hour the error would be 360 μs for an inexpensive clock, which multiplied for the velocity of ultrasound is 0.123 m. Having a bias of this magnitude in the estimated distance to one sender is not compatible with an accurate location estimation of the receiver.

In the case of GPS or Galileo satellites, the offset between two synchronized clocks (ϵ_c) is modelled as a second order polynomial [44], as follows:

$$\epsilon_c = a_0 + a_1(t - t_0) + a_2(t - t_0)^2 \tag{6.2}$$

where t_0 is a reference epoch. The values of a_0, a_1 and a_2 are broadcast from time to time to correct the satellite clocks. In our case, the a_1 value of each sender could be added to the state to estimate the drift with a first order polynomial. Another alternative would be estimate the shifts with a stationary receiver. The Kalman filter could be used, as it has been proved to be capable to track the offset and the skew of inexpensive oscillators in [45]. Lastly, the clocks could be observed and modelled during the initialization of the filter.

Bibliography

[1] Ngeletshedzo Netshidavhini and Raymond B. Mabuza. Effects of Various Couplants on Carbon Steel and Aluminium Materials Using Ultrasonic Testing. *18th World Conference on Nondestructive Testing*, 2012.

[2] G. Shen, R. Zetik, and R. S. Thoma. Performance Comparison of TOA and TDOA Based Location Estimation Algorithms in LOS Environment. *Proceedings of the 5th workshop on positioning, navigation and communication 2008 (WPNC 08)*, pages 71–78, 2008.

[3] Johannes Wendeberg, Jörg Müller, Christian Schindelhauer, and Wolfram Burgard. Robust Tracking of a Mobile Beacon using Time Differences of Arrival with Simultaneous Calibration of Receiver Positions. In *Proceedings of 2012 International Conference on Indoor Positioning and Indoor Navigation (IPIN)*, 2012.

[4] F. Gustafsson and F. Gunnarsson. Positioning using time-difference of arrival measurements. In *Acoustics, Speech, and Signal Processing, 2003. Proceedings (ICASSP'03). 2003 IEEE International Conference*, volume 6, pages VI–553, 2003.

[5] C. Hongyang, D. Ping, X. Yongjun, and L. Xiaowei. A Robust Location Algorithm with Biased Extended Kalman Filtering of TDOA Data for Wireless Sensor Networks. In *2005 International Conference on Wireless Communications, Networking and Mobile Computing, 2005. Proceedings.*, volume 2, pages 883–886. IEEE, 2005.

[6] Rui Zhang, F. Höflinger, and L.M. Reindl. TDOA based localization using Interacting Multiple Model estimator and ultrasonic transmitter/receiver. In *Systems, Signals and Devices (SSD), 2012 9th International Multi-Conference on*, pages 1–6, march 2012.

[7] K. C. Ho and Wenwei Xu. An Accurate Algebraic Solution for Moving Source Location Using TDOA and FDOA Measurements. *IEEE Transactions on Signal Processing*, 52(9):2453–2463, 2004.

[8] Yuki Takabayashi, Takashi Matsuzaki, Hiroshi Kameda, and Masayoshi Ito. Target Tracking Using TDOA/FDOA Measurements in the Distributed Sensor Network. *SICE Annual Conference*, pages 3442–3446, 2008.

[9] J.A. Cho, H. Na, S. Kim, and C. Ahn. Moving-Target Tracking Based on Particle Filter with TDOA/FDOA Measurements. *ETRI Journal*, 34(2), 2012.

[10] Ping Zou, Zhen Huang, and Jianhua Lu. Passive Stationary Target Positioning Using Adaptive Particle Filter with TDOA and FDOA Measurements. *10th Asia-Pacific Conference on Comnications and 5th International Symposium on Multi-Dimensional Hobile Comnications*, pages 453–456, 2004.

[11] K. C. Ho, Xiaoning Lu, and L. Kovavisaruch. Source Localization Using TDOA and FDOA Measurements in the Presence of Receiver Location Errors: Analysis and Solution. *IEEE Transactions on Signal Processing*, 55(2):684–696, 2007.

[12] Mathieu St-Pierre and Denis Gingras. Comparison between the unscented Kalman filter and the extended Kalman filter for the position estimation module of an integrated navigation information system. *IEEE Intelligent Vehicles Symposium, University of Parma*, pages 831–835, 2004.

[13] Khoshnam Shojaie and Alireza Mohammad Shahri. Iterated Unscented SLAM Algorithm for Navigation of an Autonomous Mobile Robot. *IEEE/RSJ International Conference on Intelligent Robots and Systems*, pages 1582–1587, 2008.

[14] Xiang Wang and Hong Zhang. A UPF-UKF Framework For SLAM. *IEEE International Conference on Robotics and Automation*, 2007.

[15] Fu-Kai Chan and Chih-Yu Wen. Adaptive AOA/TOA Localization Using Fuzzy Particle Filter for Mobile WSNs. In *Vehicular Technology Conference (VTC Spring), 2011 IEEE 73rd*, pages 1–5, 2011.

[16] J. Saloranta and G. Abreu. Solving the Fast Moving Vehicle Localization Problem via TDOA Algorithms. In *Positioning Navigation and Communication (WPNC), 2011 8th Workshop on*, pages 127–130, 2011.

[17] Patrick Hornecker. Konfigurationsfreie Lokalisierung eines mobilen Empfängers. Master's thesis, University of Freiburg, 2013.

[18] Dragana Carevic. Multisensor Tracking of An Underwater Acoustic Target. *Defence Applications of Signal Processing*, pages 1–6, 2011.

[19] Joan Bordoy, Patrick Hornecker, Fabian Höflinger, Johannes Wendeberg, Rui Zhang, Christian Schindelhauer, and Leonhard Reindl. Robust Tracking of a Mobile

Receiver using Unsynchronized Time Differences of Arrival. *International Conference on Indoor Positioning and Indoor Navigation*, 2013.

[20] Claud Powell. Early history of the Decca Navigator system. *Journal of the Institution of Electronic and Radio Engineers*, 55:203–209, 1985.

[21] C. Powell. The Decca Navigator System for Ship and Aircraft Use. *Convention on Radio Aids to Aeronautical and Marine Navigation*, (2567), 1958.

[22] N. Bowditch, National Imagery, and Mapping Agency. *The American Practical Navigator - Bowditch*. Pub. (United States. National Imagery and Mapping Agency). 2002.

[23] United States Coast Guard. LORAN-C General Information. Retrieved 18/10/2013. URL `http://www.navcen.uscg.gov/?pageName=loranMain`.

[24] Thomas Herring. Principles of the Global Positioning System . Lecture Notes, 2012. Massachusetts Institute of Technology.

[25] Kerem Ozsoy, Ayhan Bozkurt, and Ibrahim Tekin. Indoor Positioning Based on Global Positioning System Signals. *Microwave and Optical Technology Letters*, 55: 1091–1097, 2013.

[26] J. Wendeberg, T. Janson, and C. Schindelhauer. Self-Localization based on Ambient Signals. *Theoretical Computer Science*, 453:98–109, 2012.

[27] R. Biswas and S. Thrun. A Distributed Approach to Passive Localization for Sensor Networks. In *Proceedings of the National Conference on Artificial Intelligence*, volume 20, page 1248. Menlo Park, CA; Cambridge, MA; London; AAAI Press; MIT Press; 1999, 2005.

[28] T. Janson, C. Schindelhauer, and J. Wendeberg. Self-Localization Application for iPhone using only Ambient Sound Signals. In *Proceedings of the 2010 International Conference on Indoor Positioning and Indoor Navigation (IPIN)*, pages 259–268, Nov. 2010.

[29] C. Doppler. *Ueber das farbige Licht der Doppelsterne und einiger anderer Gestirne des Himmels: Versuch einer das Bradley'sche Aberrations-Theorem als integrirenden Theil in sich schliessenden allgemeineren Theorie*. Borrosch & André, 1842.

[30] Wolfram Burgard, Cyrill Stachniss, Giorgio Grisetti, Maren Bennewitz, and Christian Plagemann. Bayes Filter - Kalman Filter. Lecture Slides, 2010. University of Freiburg.

[31] Sebastian Thrun, Wolfram Burgard, and Dieter Fox. *Probabilistic Robotics*. MIT Press, 2005.

[32] Simon J Julier and Jeffrey K Uhlmann. New Extension of the Kalman Filter to Nonlinear Systems. In *AeroSense'97*, pages 182–193. International Society for Optics and Photonics, 1997.

[33] Simon J. Julier and Jeffrey K. Uhlmann. Unscented Filtering and Nonlinear Estimation. *Proceedings of the IEEE*, 92(3):401–422, 2004.

[34] Tina Toni and Bruce Tidor. Combined Model of Intrinsic and Extrinsic Variability for Computational Network Design with Application to Synthetic Biology. *PLoS Comput Biol*, 2013.

[35] Rudolph van der Merwe. Sigma-Point Kalman Filters for Probabilistic Inference in Dynamic State-Space Models. *[PhD thesis] Oregon Health & Science University*, 2004.

[36] Rudolf Geiger, Robert H. Aron, and Paul Todhunter. *The Climate Near the Ground*. Rowman & Littlefield Publishers, Inc., sixth edition, 2003.

[37] D.R. Raichel. *The Science and Applications of Acoustics*. Springer, 2010.

[38] James P. Helferty. Improved Tracking of Maneuvering Targets: The Use of Turn-Rate Distributions for Acceleration Modeling. *IEEE Transactions on Aerospace and Electronic Systems*, 32, 1996.

[39] Fernando Tusell. Kalman Filtering in R. *Journal of Statistical Software*, 39, 2011.

[40] Nicholas Assimakis, Maria Adam, and Anargyros Douladiris. Information Filter and Kalman Filter Comparison: Selection of the Faster Filter. *International Journal of Information Engineering*, 2:1–5, 2012.

[41] A.J. Dean, J.W. Langelaan, and S.N. Brennan. Improvements in terrain-based road vehicle localization by initializing an Unscented Kalman Filter using Particle Filters. *American Control Conference (ACC)*, 2010.

[42] Paolo Annibale and Rudolf Rabenstein. Speed of Sound and Air Temperature Estimation Using the TDOA-Based Localization Framework. *ICASSP*, pages 229–232, 2012.

[43] Brian Nielsen. Time in Distributed Systems. Lecture Slides, 2008. Aalborg University.

[44] J. Sanz Subirana, J.M. Juan Zornoza, and M. Hernández-Pajares. Clock Modelling, 2011. URL `http://www.navipedia.net/index.php/Clock_Modelling`.

[45] Hayang Kim, Xiaoli Ma, and Benjamin Russell Hamilton. Tracking Low-Precision Clocks With Time-Varying Drifts Using Kalman Filtering. *IEEE/ACM Transactions on Networking*, 20:257–270, 2012.